ORDER-PRESERVING INTERPOLATION FOR SUMMATION-BY-PARTS OPERATORS AT NONCONFORMING GRID INTERFACES[*]

MARTIN ALMQUIST[†], SIYANG WANG[‡], AND JONATAN WERPERS[§]

Abstract. We study nonconforming grid interfaces for summation-by-parts finite difference methods applied to partial differential equations with second derivatives in space. To maintain energy stability, previous efforts have been forced to accept a reduction of the global convergence rate by one order, due to large truncation errors at the nonconforming interface. We avoid the order reduction by generalizing the interface treatment and introducing order-preserving interpolation operators. We prove that, given two diagonal-norm summation-by-parts schemes, order-preserving interpolation operators with the necessary properties are guaranteed to exist, regardless of the grid-point distributions along the interface. The new methods retain the stability and global accuracy properties of the underlying schemes for conforming interfaces.

Key words. summation-by-parts, nonconforming interfaces, interpolation, accuracy

AMS subject classifications. 65M06, 65M12

DOI. 10.1137/18M1191609

1. Introduction. Adaptive mesh refinement is essential for efficiency in any simulation that requires high resolution in a localized area. For wave-dominated phenomena, high-order finite difference (FD) methods are often computationally efficient when the solution is smooth [12]. By combining summation-by-parts (SBP) operators [13] with simultaneous approximation terms (SATs) [4], the SBP-SAT methodology leads to energy stable and conservative high-order FD methods on multiblock and curvilinear grids [6, 27].

Mattsson and Carpenter [17] extended the SBP-SAT framework to locally refined grids by constructing SBP-preserving interpolation operators for nonconforming grid interfaces. They proved energy stability for conservation laws and parabolic equations. The approach has since been extended to the Schrödinger equation [22], the second order wave equation [31], and the advection-diffusion equation [14]. For equations with second derivatives in space, it has been observed that the SATs at the nonconforming interfaces worsen the largest local truncation error, and hence the global convergence rate, by one order, as compared to conforming interfaces [14, 21, 28]. The obvious remedy would have been to increase the order of accuracy of the interpolation operators, but [15] showed that this is impossible because the order of the interpolation operators is bounded from above by the order of the quadrature rule associated with every SBP operator [10]. Following this discovery, [7] constructed interpolation operators corresponding to novel degree-preserving first derivative SBP operators that are based on extra-high-order quadrature rules. Unlike traditional SBP FD operators,

[†]Department of Geophysics, Stanford University, Stanford, CA 94305 (malmquist@stanford.edu).

[‡]Department of Mathematical Sciences, Chalmers University of Technology and University of Gothenburg, SE-412 96 Gothenburg, Sweden (siyang.wang@chalmers.se).

[§]Department of Information Technology, Uppsala University, SE-751 05 Uppsala, Sweden (jonatan.werpers@it.uu.se).

the boundary closures of the degree-preserving operators depend on the number of grid points. It is not obvious how well this approach would extend to equations with second derivatives and variable coefficients considering the significant effort involved in constructing such SBP operators [16].

In this work we circumvent the order reduction for second order PDEs without increasing the quadrature order. Instead, we introduce new interpolation operators referred to as order-preserving (OP) interpolation operators. The key property of the OP operators is that they come in two pairs. While each pair suffers from the accuracy restriction derived in [14, 15], it is possible to avoid accuracy reduction at the interface by using particular SATs. We prove a theoretical result, which states that, given two diagonal-norm SBP operators, it is always possible to construct matching OP interpolation operators. Encouraged by this result, we construct OP operators for the special case of 2:1 grid refinement and perform numerical experiments. With these new interpolation operators, our experiments show the same global convergence rates as if the interfaces were conforming for the heat equation, the Schrödinger equation, and the second order wave equation.

SBP-preserving interpolation operators are not only used for coupling FD grid blocks of equal sizes. In [11], they were used to couple FD and discontinuous Galerkin methods, and in [14] it was shown that they are the key to coupling arbitrary SBP schemes on general meshes. In [21], interpolation operators for so-called T-junctions, i.e., grids that are nonconforming at the block level, were constructed. A recent study also coupled finite difference and finite element methods [9]. Further, [8] used SBP-preserving interpolation operators to create entropy-stable discontinuous Galerkin spectral element methods on meshes with both hanging-node and polynomial-order refinement. Although we only present experiments with FD methods, the ideas in this paper apply to hybrid methods and general node distributions.

The numerical experiments in [21] showed quite erratic convergence behavior when interpolation operators were used for the Schrödinger equation. Although the average rate was approximately as expected, the rate from one refinement level to the next varied noticeably. Numerical experiments in this paper show that erratic convergence behavior for the Schrödinger equation can be mitigated by using the same discretization of the Laplacian as for the second order wave equation.

The paper is organized as follows. We introduce some notation in section 2. In section 3 we introduce the OP operators for the Schrödinger and heat equations. In section 4 we prove that, given two SBP operators based on diagonal quadrature rules, OP interpolation operators always exist. Using OP operators, we derive an OP coupling for the second order wave equation in section 5. We then discuss three different discretizations of the Laplacian and their properties in section 6. In section 7, we present numerical experiments with the Schrödinger, heat, and second order wave equations. The OP coupling exhibits one order higher global convergence compared with previous approaches using the interpolation operators derived in [17]. We conclude in section 8.

2. Preliminaries. In this section we introduce some notation and recall the properties of second derivative SBP operators that will be needed in subsequent sections.

Let Ω denote a bounded domain in $\mathbb{R}^2$, and let $f = [f_1, \ldots, f_m]^T$ and $g = [g_1, \ldots, g_m]^T$ be vector-valued functions with m components in $C^2(\Omega)$. We will use the standard inner product and norm on $L^2(\Omega)$, i.e.,

$$(2.1) \qquad (f, g)_\Omega = \int_\Omega f^* g \, \mathrm{d}\Omega, \quad \|f\|_\Omega^2 = (f, f)_\Omega,$$

where * denotes conjugate transpose. For integration along the boundary $\partial\Omega$, we use the notation

$$\langle f, g \rangle_{\partial\Omega} = \int_{\partial\Omega} f^* g \, \mathrm{d}\Gamma.$$

We will frequently use the normal derivative on $\partial\Omega$, defined by

$$\frac{\partial f_i}{\partial\hat{n}} = \nabla f_i \cdot \hat{n},$$

where $\hat{n}$ denotes the outward unit normal. With this notation, Green's first identity reads

(2.2)
$$(f_i, \Delta g_i)_\Omega = \left\langle f_i, \frac{\partial g_i}{\partial\hat{n}} \right\rangle_{\partial\Omega} - (\nabla f_i, \nabla g_i)_\Omega.$$

Let $U = [-1, 0] \times [0, 1]$ and $V = [0, 1] \times [0, 1]$. We denote the interface between U and V by Γ. The outer boundaries are $\Gamma_U = \partial U \setminus \Gamma$ and $\Gamma_V = \partial V \setminus \Gamma$. Throughout this paper we will consider initial-boundary value problems in the form

(2.3)
$$
\begin{aligned}
L_U u &= 0, & (x, y) &\in U, & t &\in [0, T], \\
L_V v &= 0, & (x, y) &\in V, & t &\in [0, T], \\
u - v &= 0, & (x, y) &\in \Gamma, & t &\in [0, T], \\
\alpha_U \tfrac{\partial u}{\partial\hat{n}_U} + \alpha_V \tfrac{\partial v}{\partial\hat{n}_V} &= 0, & (x, y) &\in \Gamma, & t &\in [0, T], \\
B_U u &= 0, & (x, y) &\in \Gamma_U, & t &\in [0, T], \\
B_V v &= 0, & (x, y) &\in \Gamma_V, & t &\in [0, T],
\end{aligned}
$$

augmented with suitable initial conditions at time $t = 0$. Here $L_{U,V}$ are linear differential operators of second order in space and first or second order in time; $\hat{n}_{U,V}$ are outward unit normals on the interface Γ; $\alpha_{U,V}$ are scalar coefficients; and $B_{U,V}$ are boundary operators. Because our focus is on the interface treatment, we assume that the boundary operators $B_{U,V}$ are such that the problems are well-posed and will henceforth omit them in the analysis.

2.1. Summation-by-parts finite difference operators. Consider an interval $J = [x_\ell, x_r]$ and a grid vector $\mathbf{x} = [x_1, \ldots, x_N]^T$ that discretizes J. Let $F, G \in C^\infty(J)$, and let $F(\mathbf{x}) = [F(x_1), \ldots, F(x_N)]^T$ denote the restriction of F to $\mathbf{x}$. Consider a difference operator D_2 that approximates the second derivative, i.e.,

$$D_2 F(\mathbf{x}) \simeq F''(\mathbf{x}).$$

We say that D_2 has the summation-by-parts (SBP) property [20] if it can be decomposed as

$$D_2 = H^{-1}(-\widetilde{D}^T H \widetilde{D} + e_r d_r^T - e_\ell d_\ell^T),$$

where $H = H^T > 0$; $e_{\ell,r}^T$ are row vectors that interpolate to the left and right boundaries of the domain; $d_{\ell,r}^T$ are row vectors that approximate the first derivatives at the domain boundaries; and $F(\mathbf{x})^T \widetilde{D}^T H \widetilde{D} G(\mathbf{x})$ approximates $\int_J F' G' \, \mathrm{d}x$. Note that although the operator $\widetilde{D}$ is accurate in the integrated sense, $\widetilde{D}$ by itself is not necessarily an accurate approximation of the first derivative. We further require that

(2.4)
$$\widetilde{D}^T H \widetilde{D} = h\gamma(d_r d_r^T + d_\ell d_\ell^T) + \widetilde{M},$$

where γ is a positive constant and $\widetilde{M}$ is symmetric positive semidefinite. The property in (2.4) is essential for the interblock coupling in the second order wave equation [18].

Let Ω denote the unit square. We assume for ease of notation that Ω is discretized by a tensor-product grid with N grid points in each coordinate direction. Let D_2 denote an SBP operator corresponding to a single grid line, and let I denote the $N \times N$ identity matrix. On Ω, we will use the following operators:

$$
\begin{aligned}
D_{xx} &= D_2 \otimes I, & D_{yy} &= I \otimes D_2, \\
\widetilde{D}_x &= \widetilde{D} \otimes I, & \widetilde{D}_y &= I \otimes \widetilde{D}, \\
D_\Delta &= D_{xx} + D_{yy}, & H_\Omega &= H \otimes H \\
,\widetilde{M}_x &= \widetilde{M} \otimes H, & \widetilde{M}_y &= H \otimes \widetilde{M}, \\
e_{W,E} &= e_{\ell,r} \otimes I, & e_{S,N} &= I \otimes e_{\ell,r}, \\
d_W &= -d_\ell \otimes I, & d_S &= -I \otimes d_\ell, \\
d_E &= d_r \otimes I, & d_N &= I \otimes d_r.
\end{aligned}
$$

Note the minus signs in the definitions of $d_{W,S}$, which ensure that all boundary derivative operators $d_{W,S,E,N}$ approximate the outward normal derivative.

Let $\mathbf{f}$ and $\mathbf{g}$ denote the restrictions of m-valued functions $f = [f_1, \ldots, f_m]^T$ and $g = [g_1, \ldots, g_m]^T$ to the grid. We store the discrete values in $N^2 \times m$ matrices,

$$
\mathbf{f} = \begin{bmatrix} \mathbf{f}_1 & \mathbf{f}_2 & \ldots & \mathbf{f}_m \end{bmatrix}, \quad \mathbf{g} = \begin{bmatrix} \mathbf{g}_1 & \mathbf{g}_2 & \ldots & \mathbf{g}_m \end{bmatrix},
$$

where $\mathbf{f}_i$ denotes the restriction of f_i to the grid. We define the operator $\widetilde{D}_\nabla$ by

$$
\widetilde{D}_\nabla \mathbf{f}_i = \begin{bmatrix} \widetilde{D}_x \mathbf{f}_i & \widetilde{D}_y \mathbf{f}_i \end{bmatrix}.
$$

We further define a discrete inner product in $\mathbb{C}^{N^2 \times m}$ and a corresponding norm,

$$
(2.5) \qquad (\mathbf{f}, \mathbf{g}) = \sum_{i=1}^{m} \mathbf{f}_i^* H_\Omega \mathbf{g}_i, \quad \|\mathbf{f}\|^2 = (\mathbf{f}, \mathbf{f}).
$$

Notice that (2.5) approximates (2.1). For boundary integrals we use the notation

$$
(2.6) \qquad \langle e_W^T \mathbf{f}_i, e_W^T \mathbf{g}_i \rangle = (e_W^T \mathbf{f}_i)^* H (e_W^T \mathbf{g}_i)
$$

and

$$
\langle\!\langle e_W^T \mathbf{f}_i \rangle\!\rangle^2 = \langle e_W^T \mathbf{f}_i, e_W^T \mathbf{f}_i \rangle.
$$

Because of the SBP properties, the discrete operators satisfy a discrete version of Green's identity (2.2),

$$
(2.7) \qquad (\mathbf{f}_i, D_\Delta \mathbf{g}_i) = -\left(\widetilde{D}_\nabla \mathbf{f}_i, \widetilde{D}_\nabla \mathbf{g}_i \right) + \sum_{\alpha \in \{W,S,E,N\}} \langle e_\alpha^T \mathbf{f}_i, d_\alpha^T \mathbf{g}_i \rangle.
$$

Because of the property in (2.4) we have

$$
(2.8) \qquad \left(\widetilde{D}_\nabla \mathbf{f}_i, \widetilde{D}_\nabla \mathbf{g}_i \right) = \mathbf{f}_i^* (\widetilde{M}_x + \widetilde{M}_y) \mathbf{g}_i + \sum_{\alpha \in \{W,S,E,N\}} h\gamma \langle d_\alpha^T \mathbf{f}_i, d_\alpha^T \mathbf{g}_i \rangle,
$$

where $\widetilde{M}_{x,y}$ are symmetric positive semidefinite.

2.2. Notation for two-block discretizations. Consider the two-block problem (2.3). Let $\mathbf{u}$ and $\mathbf{v}$ approximate u and v, respectively. In each grid block we introduce SBP FD operators in the way described in the previous section. The operators could be based on different numbers of grid points or different orders of accuracy and are hence not identical, in general. For notational convenience, however, we will not use different symbols for the differential operators, e.g., D_Δ. But in this setting it is important to distinguish between the different quadratures that are used in the two blocks. Let H_U^Γ denote the one-dimensional quadrature matrix H used in U, and let H_V^Γ denote the quadrature matrix in V. The corresponding two-dimensional quadrature matrices are

$$H_U = H_U^\Gamma \otimes H_U^\Gamma, \quad H_V = H_V^\Gamma \otimes H_V^\Gamma.$$

We will write $(\cdot, \cdot)_U$ for the inner product used in U, and $(\cdot, \cdot)_V$ for the inner product in V. Similarly, the boundary integrals corresponding to (2.6) will be denoted by $\langle \cdot, \cdot \rangle_U$ and $\langle \cdot, \cdot \rangle_V$. Using the SBP formula (2.7) for U and V we can write

$$(2.9) \qquad (\mathbf{u}, D_\Delta \phi)_U = \left\langle e_E^T \mathbf{u}, d_E^T \phi \right\rangle_U - \left(\widetilde{D}_\nabla \mathbf{u}, \widetilde{D}_\nabla \phi \right)_U$$

and

$$(2.10) \qquad (\mathbf{v}, D_\Delta \psi)_V = \left\langle e_W^T \mathbf{v}, d_W^T \psi \right\rangle_V - \left(\widetilde{D}_\nabla \mathbf{v}, \widetilde{D}_\nabla \psi \right)_V.$$

Here, we have ignored all boundary terms not belonging to the interface between U and V since they do not enter the stability analysis of the interface treatment. They should be taken care of by proper enforcement of well-posed boundary conditions.

Similarly, the property in (2.8) leads to

$$(2.11) \qquad \left(\widetilde{D}_\nabla \mathbf{u}, \widetilde{D}_\nabla \boldsymbol{\varphi} \right)_U = h_u \gamma_u \left\langle d_E^T \mathbf{u}, d_E^T \boldsymbol{\varphi} \right\rangle_U + \mathbf{u}^* \left(\widetilde{M}_x + \widetilde{M}_y \right) \boldsymbol{\varphi}$$

and

$$(2.12) \qquad \left(\widetilde{D}_\nabla \mathbf{v}, \widetilde{D}_\nabla \boldsymbol{\psi} \right)_V = h_v \gamma_v \left\langle d_W^T \mathbf{v}, d_W^T \boldsymbol{\psi} \right\rangle_V + \mathbf{v}^* \left(\widetilde{M}_x + \widetilde{M}_y \right) \boldsymbol{\psi},$$

where $h_{u,v}$ denote the grid spacings and the constants $\gamma_{u,v}$ correspond to the (possibly different) SBP operators used in U and V.

3. Parabolic and Schrödinger-type equations. In this section we consider initial-boundary value problems of the form

$$(3.1) \qquad \begin{aligned} u_t - a\Delta u &= 0, & (x,y) &\in U, & t &\in [0, T], \\ v_t - b\Delta v &= 0, & (x,y) &\in V, & t &\in [0, T], \\ u - v &= 0, & (x,y) &\in \Gamma, & t &\in [0, T], \\ a\frac{\partial u}{\partial \hat{n}_U} + b\frac{\partial v}{\partial \hat{n}_V} &= 0, & (x,y) &\in \Gamma, & t &\in [0, T], \end{aligned}$$

with initial data for u and v. We assume that a and b are constant coefficients with nonnegative real parts. If a and b are real and positive, (3.1) is a parabolic problem. Purely imaginary a and b yield a Schrödinger-type problem.

Before discretizing (3.1), we derive an energy estimate for the continuous problem. Multiplying the first equation in (3.1) by u^* and integrating over U yields

$$(u, u_t)_U = a(u, \Delta u)_U = a \left\langle u, \frac{\partial u}{\partial \hat{n}_U} \right\rangle_{\partial U} - a\|\nabla u\|_U^2 = a \left\langle u, \frac{\partial u}{\partial \hat{n}_U} \right\rangle_\Gamma - a\|\nabla u\|_U^2,$$

where we discarded terms related to outer boundaries in the last step. By repeating the procedure on V and using the interface conditions, we obtain the estimate

$$\frac{\mathrm{d}}{\mathrm{d}t}\left(\|u\|_U^2 + \|v\|_V^2\right) = -(a + a^*)\|\nabla u\|_U^2 - (b + b^*)\|\nabla v\|_V^2.$$

3.1. Semidiscrete approximation. The semidiscrete approximation of (3.1) can be written as

$$(3.2) \qquad \begin{aligned} \mathbf{u}_t - aD_\Delta \mathbf{u} &= SAT_u, \\ \mathbf{v}_t - bD_\Delta \mathbf{v} &= SAT_v, \end{aligned}$$

where $SAT_{u,v}$ are penalty terms that weakly impose the interface conditions on Γ. For notational convenience we write, e.g., $\mathbf{u}_t$ for $\frac{\mathrm{d}\mathbf{u}}{\mathrm{d}t}$. We make the ansatz

$$SAT_u = \tau_u a^* H_U^{-1} d_E H_U^\Gamma (e_E^T \mathbf{u} - I_{v2u}^g e_W^T \mathbf{v}) + \sigma_u H_U^{-1} e_E H_U^\Gamma (ad_E^T \mathbf{u} + I_{v2u}^b bd_W^T \mathbf{v}),$$
$$SAT_v = \tau_v b^* H_V^{-1} d_W H_V^\Gamma (e_W^T \mathbf{v} - I_{u2v}^g e_E^T \mathbf{u}) + \sigma_v H_V^{-1} e_W H_V^\Gamma (bd_W^T \mathbf{v} + I_{u2v}^b ad_E^T \mathbf{u}),$$

where $\tau_{u,v}$ and $\sigma_{u,v}$ are scalar penalty parameters. The interpolation operators $I_{v2u}^{g,b}$ and $I_{u2v}^{g,b}$ interpolate between the two different grids that discretize the interface Γ. For now, the superscripts g and b simply indicate that we allow different interpolation operators for the four penalty terms. As will be evident in the following subsection there will be two "good" and two "bad" operators, hence the choice of letters. In the case of matching grids (and matching quadratures), all the interpolation operators can be replaced by identity matrices. Note that the above ansatz is more general than those used for the Schrödinger equation in [22] and parabolic equations in [17]. The extra generality is what will enable us to obtain higher order of accuracy. The above ansatz reduces to the ones in [17, 22] if we set

$$I_{v2u}^g = I_{v2u}^b, \quad I_{u2v}^g = I_{u2v}^b.$$

In the following subsection we analyze the local truncation errors introduced by $SAT_{u,v}$ in (3.2), to determine what accuracies we require of the different interpolation operators. After that, we derive stability conditions on the interpolation operators.

3.2. Local truncation errors and convergence rates. Let $\mathbf{x}_u$ and $\mathbf{x}_v$ be two different grid vectors that discretize an interval J. Let f be a smooth function, and let $\mathbf{f}_u$ and $\mathbf{f}_v$ denote its restrictions to $\mathbf{x}_u$ and $\mathbf{x}_v$, respectively. If I_{u2v} and I_{v2u} are interpolation operators of orders q_{u2v} and q_{v2u}, then

$$(3.3) \qquad \begin{aligned} I_{u2v}\mathbf{f}_u &= \mathbf{f}_v + \mathcal{O}(h^{q_{u2v}}), \\ I_{v2u}\mathbf{f}_v &= \mathbf{f}_u + \mathcal{O}(h^{q_{v2u}}), \end{aligned}$$

where the interpolation error in (3.3) denotes the maximum error over all grid points.

Traditional diagonal-norm SBP operators [16, 20] with $2p$th order of accuracy in the interior are of order p at a fixed number of near-boundary grid points. In two dimensions, all grid points near an interface or boundary are affected by the pth order errors. Still, for equations with second derivatives in space, numerical experiments often show $\min(2p, p + 2)$th order convergence rates. For one-dimensional problems, a general normal mode analysis shows that the convergence rate of pointwise stable schemes is at least $\min(2p, p + 2)$ [26]. A detailed analysis of a class of SBP–SAT discretizations for the second order wave equation proves that, with properly chosen

penalty parameter, the convergence rate sometimes exceeds $\min(2p, p+2)$ [29]. This result is extended to two-dimensional problems in [30]. However, when conforming grid interfaces are present the rate does not exceed $\min(2p, p+2)$, in general. We will refer to $\min(2p, p+2)$ as the ideal rate that we hope to preserve when using interpolation operators at nonconforming interfaces.

The boundary derivative operators $d_{W,E,S,N}^T$ are typically constructed to be of order $p+1$ to ensure that SATs at boundaries and conforming interfaces do not cause truncation errors of order less than p. Hence, we can ignore their effect in this discussion. To analyze the local truncation errors of the SATs, we let $\mathbf{w}_{u,v}$ denote the restrictions of the exact solution to the grids on the left and right sides of the interface. Assume that, e.g., I_{u2v}^g is of order q_{u2v}^g. The truncation errors are

$$
\begin{aligned}
T_u = \tau_u a^* \underbrace{H_U^{-1} d_E H_U^\Gamma}_{\sim h^{-2}} \underbrace{(e_E^T \mathbf{w}_u - I_{v2u}^g e_W^T \mathbf{w}_v)}_{\sim h^{q_{v2u}^g}} \\
+ \sigma_u \underbrace{H_U^{-1} e_E H_U^\Gamma}_{\sim h^{-1}} \underbrace{(a d_E^T \mathbf{w}_u + I_{v2u}^b b d_W^T \mathbf{w}_v)}_{\sim h^{q_{v2u}^b}} \\
= \mathcal{O}(h^{q_{v2u}^g - 2}) + \mathcal{O}(h^{q_{v2u}^b - 1})
\end{aligned}
$$

and

$$
\begin{aligned}
T_v = \tau_v b^* \underbrace{H_V^{-1} d_W H_V^\Gamma}_{\sim h^{-2}} \underbrace{(e_W^T \mathbf{w}_v - I_{u2v}^g e_E^T \mathbf{w}_u)}_{\sim h^{q_{u2v}^g}} \\
+ \sigma_v \underbrace{H_V^{-1} e_W H_V^\Gamma}_{\sim h^{-1}} \underbrace{(b d_W^T \mathbf{w}_v + I_{u2v}^b a d_E^T \mathbf{w}_u)}_{\sim h^{q_{v2u}^b}} \\
= \mathcal{O}(h^{q_{u2v}^g - 2}) + \mathcal{O}(h^{q_{u2v}^b - 1}).
\end{aligned}
$$

Note that to balance the errors from the different interpolation operators we require

$$
q_{u2v}^g = q_{v2u}^g = q_{u2v}^b + 1 = q_{v2u}^b + 1.
$$

That is, I_{u2v}^g and I_{v2u}^g should ideally be one order more accurate than I_{u2v}^b and I_{v2u}^b.

Suppose that diagonal-norm SBP operators of interior order $2p$ are used on both sides of the interface. The inner product matrices of traditional SBP FD operators of interior accuracy $2p$ correspond to quadrature rules of order $2p$ [10]. As will be discussed in more detail in section 4, the order of the inner product matrix is what limits the accuracy of the interpolation operators. The highest achievable accuracy turns out to be

$$
q_{u2v}^g = q_{v2u}^g = p + 1, \quad q_{u2v}^b = q_{v2u}^b = p,
$$

which leads to

$$
T_{u,v} = \mathcal{O}(h^{p-1}).
$$

Recall that the diagonal-norm SBP derivative operators have accuracy p at all grid points along the interface. Ideally we would have wanted $T_{u,v} = \mathcal{O}(h^p)$, but since that is impossible, the best we can do is to construct interpolation operators such that $T_{u,v} = \mathcal{O}(h^{p-1})$ only at $\mathcal{O}(1)$ grid points along the interface. It is not obvious how the global convergence rate will be affected by a localized large truncation error. Because the error is more localized than that of the derivative operators, one would expect at least $(p+1)$th order global convergence, but could hope for higher order.

Indeed, we observe $(p+2)$th order global convergence for $p = 2, 3$ in the numerical experiments in section 7.

In the less general interface coupling with

$$I_{u2v}^g = I_{u2v}^b = I_{u2v}, \quad I_{v2u}^g = I_{v2u}^b = I_{v2u},$$

we obtain local truncation errors

$$T_u = \mathcal{O}(h^{q_{v2u}-2}), \quad T_v = \mathcal{O}(h^{q_{u2v}-2}).$$

The stability requirements on the interpolation operators limit the accuracies according to (see [14])

$$q_{u2v} + q_{v2u} \leq 2p + 1.$$

In this case, it is inevitable that $\max(T_u, T_v) = \mathcal{O}(h^{p-2})$. Hence, with the new OP coupling, the largest local truncation error is one order higher than the largest local truncation error in previous approaches. Therefore, it is reasonable to expect an improvement by one order in global convergence rate.

3.3. Stability. The aim in this subsection is to derive conditions for energy stability on the interpolation operators. The error analysis in the previous subsection showed that all the SATs in (3.2) give truncation errors of equal order if the "good" interpolation operators, $I_{\cdot 2 \cdot}^g$, are one order more accurate than the "bad" ones, $I_{\cdot 2 \cdot}^b$.

To analyze stability we multiply the first and second equations in (3.2) by $\mathbf{u}^* H_U$ and $\mathbf{v}^* H_V$, respectively, which leads to

$$(\mathbf{u}, \mathbf{u}_t)_U = a\,(\mathbf{u}, D_\Delta \mathbf{u})_U + (\mathbf{u}, SAT_u)_U\,,$$
$$(\mathbf{v}, \mathbf{v}_t)_V = b\,(\mathbf{v}, D_\Delta \mathbf{v})_V + (\mathbf{v}, SAT_v)_V\,.$$

Using the SBP formulas (2.9) and (2.10), we obtain

$$a\,(\mathbf{u}, D_\Delta \mathbf{u})_U = a\,\langle e_E^T \mathbf{u}, d_E^T \mathbf{u}\rangle_U - a\left(\widetilde{D}_\nabla \mathbf{u}, \widetilde{D}_\nabla \mathbf{u}\right)_U$$
$$= a\,\langle e_E^T \mathbf{u}, d_E^T \mathbf{u}\rangle_U - a\|\widetilde{D}_\nabla \mathbf{u}\|_U^2,$$

and similarly

$$b\,(\mathbf{v}, D_\Delta \mathbf{v})_V = b\,\langle e_W^T \mathbf{v}, d_W^T \mathbf{v}\rangle_V - b\|\widetilde{D}_\nabla \mathbf{v}\|_V^2.$$

The SATs yield

$$(\mathbf{u}, SAT_u)_U = \tau_u a^* \langle d_E^T \mathbf{u}, e_E^T \mathbf{u} - I_{v2u}^g e_W^T \mathbf{v}\rangle_U + \sigma_u \langle e_E^T \mathbf{u}, a d_E^T \mathbf{u} + I_{v2u}^b b d_W^T \mathbf{v}\rangle_U,$$
$$(\mathbf{v}, SAT_v)_V = \tau_v b^* \langle d_W^T \mathbf{v}, e_W^T \mathbf{v} - I_{u2v}^g e_E^T \mathbf{u}\rangle_V + \sigma_v \langle e_W^T \mathbf{v}, b d_W^T \mathbf{v} + I_{u2v}^b a d_E^T \mathbf{u}\rangle_V.$$

We can now conclude that the discrete energy rate is

$$\frac{\mathrm{d}}{\mathrm{d}t}\left(\|\mathbf{u}\|_U^2 + \|\mathbf{v}\|_V^2\right) = -(a+a^*)\|\widetilde{D}_\nabla \mathbf{u}\|_U^2 - (b+b^*)\|\widetilde{D}_\nabla \mathbf{v}\|_V^2 + w^* A w,$$

where we have defined

$$w = \begin{bmatrix} e_E^T \mathbf{u} \\ e_W^T \mathbf{v} \\ d_E^T \mathbf{u} \\ d_W^T \mathbf{v} \end{bmatrix}, \quad A = \begin{bmatrix} & & \alpha_{13} & \alpha_{14} \\ & & \alpha_{23} & \alpha_{24} \\ \alpha_{13}^* & \alpha_{23}^* & & \\ \alpha_{14}^* & \alpha_{24}^* & & \end{bmatrix},$$

and

$$
\begin{aligned}
\alpha_{13} &= \left(a + a\tau_u^* + a\sigma_u\right) H_U^\Gamma, \\
\alpha_{14} &= b\sigma_u H_U^\Gamma I_{v2u}^b - b\tau_v^* (I_{u2v}^g)^* H_V^\Gamma, \\
\alpha_{23} &= -a\tau_u^* (I_{v2u}^g)^* H_U^\Gamma + a\sigma_v H_V^\Gamma I_{u2v}^b, \\
\alpha_{24} &= (b + b\tau_v^* + b\sigma_v) H_V^\Gamma.
\end{aligned}
\tag{3.4}
$$

The matrix A is symmetric and has zeros on the diagonal. To ensure that $w^* A w$ is nonpositive we need all the elements of A to vanish. When the grids are conforming and the same SBP operators are used in U and V, all interpolation operators can be replaced by identity matrices and the inner products are the same, i.e., $H_U^\Gamma = H_V^\Gamma$. The stability conditions then reduce to

$$
\begin{aligned}
1 + \tau_u^* + \sigma_u &= 0, \\
\sigma_u - \tau_v^* &= 0, \\
-\tau_u^* + \sigma_v &= 0, \\
1 + \tau_v^* + \sigma_v &= 0,
\end{aligned}
\tag{3.5}
$$

which is equivalent to

$$
\begin{aligned}
1 + \tau_u^* + \tau_v^* &= 0, \\
\sigma_u &= \tau_v^*, \\
\sigma_v &= \tau_u^*.
\end{aligned}
$$

There is one free parameter, but the only solution that treats the left and right directions identically is [2, 22]

$$
\tau_u = \sigma_u = \tau_v = \sigma_v = -1/2.
\tag{3.6}
$$

Now we return to the general case of nonconforming grids. Assume that the interpolation operators have the properties

$$
\begin{aligned}
H_U^\Gamma I_{v2u}^b &= (I_{u2v}^g)^* H_V^\Gamma, \\
(I_{v2u}^g)^* H_U^\Gamma &= H_V^\Gamma I_{u2v}^b.
\end{aligned}
\tag{3.7}
$$

Then, by substituting (3.7) in (3.4), we find that the condition that all entries of A equal zero again reduces to (3.5) and the parameter values in (3.6) yield stability. The stability condition (3.7) relates I_{v2u}^b to I_{u2v}^g and I_{u2v}^b to I_{v2u}^g. Thus, we may use two pairs of operators that are unrelated to one another.

3.4. The stability condition in terms of Hilbert adjoints. Let N_U and N_V denote the number of grid points along the interface in U and V, respectively. The matrices H_U^Γ and H_V^Γ define inner products in $\mathbb{C}^{N_U}$ and $\mathbb{C}^{N_V}$ by

$$
(\mathbf{u}_\Gamma, \boldsymbol{\phi}_\Gamma)_{U_\Gamma} = \mathbf{u}_\Gamma^* H_U^\Gamma \boldsymbol{\phi}_\Gamma, \quad (\mathbf{v}_\Gamma, \boldsymbol{\psi}_\Gamma)_{V_\Gamma} = \mathbf{v}_\Gamma^* H_V^\Gamma \boldsymbol{\psi}_\Gamma.
$$

Let the resulting inner product spaces be denoted by U_Γ and V_Γ. It follows from the completeness of $\mathbb{C}$ that also U_Γ and V_Γ are complete, and hence Hilbert spaces. By definition, the Hilbert adjoint $L^\dagger$ of a linear operator $L : U_\Gamma \mapsto V_\Gamma$ satisfies

$$
(v, Lu)_{V_\Gamma} = (L^\dagger v, u)_{U_\Gamma} \quad \forall\, u \in U_\Gamma, v \in V_\Gamma.
\tag{3.8}
$$

Linear operators from $\mathbb{C}^m$ to $\mathbb{C}^n$ are represented by rectangular matrices, and hence (3.8) is equivalent to the condition

$$H_V^\Gamma L = (L^\dagger)^* H_U^\Gamma.$$

We note that the stability condition (3.7) can be equivalently written as

$$
\begin{aligned}
(3.9) \qquad\qquad I_{v2u}^b &= (I_{u2v}^g)^\dagger, \\
I_{v2u}^g &= (I_{u2v}^b)^\dagger.
\end{aligned}
$$

To obtain a stable scheme, it is enough to choose two interpolation operators, say I_{v2u}^g and I_{u2v}^g. The two remaining operators I_{u2v}^b and I_{v2u}^b are uniquely determined as the adjoints of the first two operators. But for the scheme to be accurate, both I_{v2u}^g and I_{u2v}^g, as well as their adjoints, must be accurate interpolation operators. Naturally, the stability condition (3.9) is also essential for dual-consistent (or adjoint-consistent) discretizations with nonconforming grids.

Let $q(I)$ denote the order of accuracy of an interpolation operator I. Based on the stability and accuracy analysis in this section, we introduce the following definition.

DEFINITION 3.1. *Given two inner product matrices H_U^Γ and H_V^Γ that correspond to quadrature rules of order $2p$, we say that the interpolation operators I_{u2v}^g, I_{u2v}^b, I_{v2u}^g, and I_{v2u}^b constitute a set of order-preserving interpolation operators if*

$$
\begin{aligned}
I_{v2u}^b &= (I_{u2v}^g)^\dagger, \\
I_{v2u}^g &= (I_{u2v}^b)^\dagger,
\end{aligned}
$$

and

$$
\begin{aligned}
q\left(I_{u2v}^g\right) = q\left(I_{v2u}^g\right) &= p+1, \\
q\left(I_{u2v}^b\right) = q\left(I_{v2u}^b\right) &= p.
\end{aligned}
$$

The order-preserving (OP) operators are defined so that the scheme (3.2) is stable with truncation error of order $p-1$ in maximum norm.

4. Existence of interpolation operators. In this section we will restate the known results that bound the sum of the orders of the interpolation operators I_{u2v} and $I_{v2u} = I_{u2v}^\dagger$ from above. As an example, in the case of traditional SBP operators with $2p$th order interior stencils on both sides of the interface, the bound is

$$(4.1) \qquad\qquad q(I_{u2v}) + q(I_{v2u}) \leq 2p+1.$$

It is important to note that the sum of the orders is an odd number. When using only one adjoint pair of interpolation operators, the global order will be dictated by $\min(q(I_{u2v}), q(I_{v2u}))$, which cannot exceed p [14]. Hence, previous approaches [14, 17, 21, 28] have not had a reason to let $\max(q(I_{u2v}), q(I_{v2u})) = p+1$. The OP approach with two pairs of operators utilizes the extra order to improve the global convergence rate.

After restating the known results we present a new theorem that shows that the bounds similar to (4.1) are always sharp. That is, one can always construct an adjoint pair $I_{u2v} = I_{v2u}^\dagger$ with the maximal accuracy allowed by the bounds. Further, the total order of accuracy may be divided arbitrarily between I_{u2v} and I_{v2u}. Guided by the new existence result, we proceed to construct new OP interpolation operators for the special case of a 2:1 grid size ratio and $2p$th order interior stencils on both sides for $2p = 2, 4, 6, 8$.

4.1. Theoretical results. Consider two vectors $\mathbf{x}_u = [x_1, \ldots, x_{N_u}]^T$ and $\mathbf{x}_v = [\xi_1, \ldots, \xi_{N_v}]^T$ that discretize an interval $J = [\alpha, \beta]$. For monomials x^j, $j \geq 0$, we write, e.g., $\mathbf{x}_u^j = [x_1^j, \ldots, x_{N_u}^j]^T$. Consider two inner product matrices $H_{u,v}$. In this section we use the inner product notation

$$(\mathbf{u}, \boldsymbol{\varphi})_u = \mathbf{u}^* H_u \boldsymbol{\varphi}, \quad (\mathbf{v}, \boldsymbol{\psi})_v = \mathbf{v}^* H_v \boldsymbol{\psi}.$$

We also introduce Vandermonde-like matrices

$$X_u^{m,n} = [\mathbf{x}_u^m, \mathbf{x}_u^{m+1}, \ldots, \mathbf{x}_u^n].$$

Assume that the inner product matrices $H_{u,v}$ correspond to quadrature rules of orders $q_{u,v}$ on $\mathbf{x}_{u,v}$. This means that $H_{u,v}$ integrate polynomials of degree less than $q_{u,v}$ exactly, i.e.,

$$(4.2) \qquad \left(\mathbf{x}_u^i, \mathbf{x}_u^j\right)_u = \frac{1}{i+j+1}(\beta^{i+j+1} - \alpha^{i+j+1}), \quad i+j < q_u,$$

and similarly for H_v. We also assume that the orders are not in fact higher than $q_{u,v}$, i.e.,

$$\left(\mathbf{x}_u^i, \mathbf{x}_u^j\right)_u \neq \frac{1}{i+j+1}(\beta^{i+j+1} - \alpha^{i+j+1}), \quad i+j = q_u,$$

with similar conditions for H_v. In the case $q_u = q_v = q$, we assume that H_u and H_v do not have the same leading order error, i.e.,

$$\left(\mathbf{x}_u^i, \mathbf{x}_u^j\right)_u \neq \left(\mathbf{x}_v^i, \mathbf{x}_v^j\right)_v, \quad i+j = q.$$

This condition is justifiable in practice. Consider, for example, the case when H_u and H_v are based on the same quadrature formula but with different numbers of grid points, e.g., $N_u > N_v$. Then we expect H_u to have a smaller truncation error than H_v, and hence the leading order error terms will not be equal.

The order conditions (4.2) imply that

$$(X_u^{0,i})^T H_u X_u^{0,j} = (X_v^{0,i})^T H_v X_v^{0,j}, \quad i+j = \min(q_u, q_v) - 1,$$

because both H_u and H_v are exact quadratures for polynomials of degree less than $\min(q_u, q_v)$. An interpolation operator I_{u2v} is accurate of order q if it is exact for polynomials of degree up to $q - 1$, i.e.,

$$I_{u2v} X_u^{0,q-1} = X_v^{0,q-1}.$$

The first important theorem is due to Lundquist, Malan, and Nordström [14].

THEOREM 4.1. *If $I_{v2u} = I_{u2v}^\dagger$, then*

$$q(I_{u2v}) + q(I_{v2u}) \leq \min(q_u, q_v) + 1.$$

Proof. See [14]. □

A proof of Theorem 4.1 for the special case $q_u = q_v$ first appeared in [15].

The following theorem shows that, given two inner product matrices, it is always possible to construct an adjoint pair $I_{v2u} = I_{u2v}^\dagger$ with the maximal accuracy allowed by Theorem 4.1.

THEOREM 4.2. *Let q_{u2v} and q_{v2u} be integers such that $1 \leq q_{u2v} \leq N_u$, $1 \leq q_{v2u} \leq N_v$ and*

$$q_{u2v} + q_{v2u} \leq \min(q_u, q_v) + 1.$$

Then there exists I_{u2v} such that we may set $I_{v2u} = I_{u2v}^{\dagger}$ and obtain

$$q(I_{u2v}) = q_{u2v}, \quad q(I_{v2u}) = q_{v2u}.$$

Proof. We seek I_{u2v} such that $q(I_{u2v}) = q_{u2v}$, i.e.,

$$(4.3) \qquad I_{u2v} X_u^{0,\,q_{u2v}-1} = X_v^{0,\,q_{u2v}-1}.$$

Upon setting $I_{v2u} = I_{u2v}^{\dagger}$, the condition that $q(I_{v2u}) = q_{v2u}$ yields

$$X_u^{0,\,q_{v2u}-1} = I_{v2u} X_v^{0,\,q_{v2u}-1} = I_{u2v}^{\dagger} X_v^{0,\,q_{v2u}-1} = H_u^{-1} I_{u2v}^T H_v X_v^{0,\,q_{v2u}-1},$$

which we may write as

$$(4.4) \qquad I_{u2v}^T H_v X_v^{0,\,q_{v2u}-1} = H_u X_u^{0,\,q_{v2u}-1}.$$

Thus, we are seeking an operator I_{u2v} that satisfies the two accuracy conditions (4.3) and (4.4). At this point, we require the assumption that $N_u \geq q_{u2v}$, i.e., that there are sufficiently many grid points. We organize the remainder of the proof into two parts. First, we show that the result holds in the case $N_u = q_{u2v}$. Second, we prove the result for $N_u > q_{u2v}$.

Assume that $N_u = q_{u2v}$. In this case, $X_u^{0,q_{u2v}-1} = V_u^{q_{u2v}}$, where V_u^n denotes the Vandermonde matrix of order n. The Vandermonde matrix is square and invertible, so the first accuracy condition (4.3) determines I_{u2v} uniquely:

$$I_{u2v} = X_v^{0,\,q_{u2v}-1}(V_u^{q_{u2v}})^{-1}.$$

Substituting the expression for I_{u2v} in the second condition (4.4) yields

$$(V_u^{q_{u2v}})^{-T}(X_v^{0,\,q_{u2v}-1})^T H_v X_v^{0,\,q_{v2u}-1} = H_u X_u^{0,\,q_{v2u}-1},$$

which is equivalent to

$$(4.5) \qquad (X_v^{0,\,q_{u2v}-1})^T H_v X_v^{0,\,q_{v2u}-1} = (X_u^{0,\,q_{u2v}-1})^T H_u X_u^{0,\,q_{v2u}-1}.$$

If (4.5) is satisfied, then I_{u2v} and $I_{u2v}^{\dagger}$ are accurate of orders q_{u2v} and q_{v2u}. But (4.5) is satisfied for any q_{u2v}, q_{v2u} such that $q_{u2v} + q_{v2u} \leq \min(q_u, q_v) + 1$, because both quadrature matrices integrate such polynomials exactly.

It remains to prove that we can find I_{u2v} with the desired accuracy properties when $N_u > q_{u2v}$. To obtain an invertible matrix in the left-hand side of (4.3) we can pad the system with extra equations in which the right-hand side is arbitrary, i.e.,

$$(4.6) \qquad I_{u2v} V_u^{N_u} = \widetilde{X}_v^{q_{u2v}-1} = \begin{bmatrix} X_v^{0,\,q_{u2v}-1} & \widetilde{X}_v \end{bmatrix},$$

where the entries of $\widetilde{X}_v$ are arbitrary. The columns of $\widetilde{X}_v$ are the results of applying I_{u2v} to polynomials of degree larger than or equal to q_{u2v}, which we do not need to put any conditions on. By solving (4.6) for I_{u2v} and substituting in the second condition (4.4), we arrive at the system

$$(4.7) \qquad (\widetilde{X}_v^{q_{u2v}-1})^T H_v X_v^{0,\,q_{v2u}-1} = (V_u^{N_u})^T H_u X_u^{0,\,q_{v2u}-1},$$

and we must prove that there exists $\widetilde{X}_v$ that satisfies this equation. Using the block structure of $\widetilde{X}_v^{q_{u2v}-1}$ and $V_u^{N_u}$, (4.7) can be written as

$$\begin{bmatrix} (X_v^{0,\,q_{u2v}-1})^T H_v X_v^{0,\,q_{v2u}-1} \\ \widetilde{X}_v^T H_v X_v^{0,\,q_{v2u}-1} \end{bmatrix} = \begin{bmatrix} (X_u^{0,\,q_{u2v}-1})^T H_u X_u^{0,\,q_{v2u}-1} \\ (X_u^{q_{u2v},\,N_u-1})^T H_u X_u^{0,\,q_{v2u}-1} \end{bmatrix}.$$

The upper system of equations is again satisfied if $q_{u2v}+q_{v2u} \leq \min(q_u, q_v)+1$ because both quadrature matrices integrate such polynomials exactly. It remains to show that we can find $\widetilde{X}_v$ that satisfies

$$\widetilde{X}_v^T H_v X_v^{0,\,q_{v2u}-1} = (X_u^{q_{u2v},\,N_u-1})^T H_u X_u^{0,\,q_{v2u}-1}.$$

Let $A = (X_v^{0,\,q_{v2u}-1})^T H_v$ and $B = (X_u^{0,\,q_{v2u}-1})^T H_u X_u^{q_{u2v},\,N_u-1}$ so that the system can be written as

$$A\widetilde{X}_v = B,$$

where $A \in \mathbb{R}^{q_{v2u} \times N_v}$. A sufficient condition for a solution matrix $\widetilde{X}_v$ to exist is that A has full row rank. Because

$$\mathrm{rank}(H_v) = N_v, \quad \mathrm{rank}(X_v^{0,\,q_{v2u}-1}) = \min(q_{v2u}, N_v),$$

it follows that

$$\mathrm{rank}(A) = \min(q_{v2u}, N_v).$$

Hence, A has full row rank if $N_v \geq q_{v2u}$. This proves the theorem. $\qquad\square$

Remark 4.3. Let $\min(q_u, q_v) = 2p$. By Theorem 4.1, $q(I_{u2v}) + q(I_{v2u}) \leq 2p + 1$. Theorem 4.2 guarantees that interpolation operator pairs such that $q(I_{u2v})+q(I_{v2u}) = 2p + 1$ exist. Further, it shows that we may distribute the total order of $2p + 1$ freely. In this paper, we are only interested in operators such that

$$q(I_{u2v}) = p + 1, \quad q(I_{v2u}) = p,$$

or

$$q(I_{u2v}) = p, \quad q(I_{v2u}) = p + 1,$$

because these choices lead to a balance of truncation errors in the numerical scheme. However, operator pairs such that, e.g.,

$$q(I_{u2v}) = p + 2, \quad q(I_{v2u}) = p - 1$$

are also guaranteed to exist.

Remark 4.4. Note that Theorem 4.2 only concerns the interpolation error in maximum norm. For finite volume, finite element, and discontinuous Galerkin methods, for example, this is all that matters. However, to obtain the ideal convergence rate with traditional FD methods we require the interpolation operators to have smaller ℓ^2-errors than the pointwise errors guaranteed by Theorem 4.2. That is, the interpolation operators should be accurate of orders q_{u2v} and q_{v2u} at $\mathcal{O}(1)$ grid points only, and at least one order more accurate at remaining grid points. Theorem 4.2 does not guarantee that such operators exist. In our experience, however, it is not difficult to obtain high order for the interior grid points where the quadrature weights are constant.

4.2. Examples of order-preserving interpolation operators. For the numerical experiments in section 7, we have constructed OP interpolation operators for the special case of a 2:1 grid size ratio and $2p$th order interior stencils on both sides for $2p = 2, 4, 6, 8$. They are compatible with diagonal-norm SBP operators with minimal number of boundary points on equidistant grids; see, e.g., [25]. Actually, they are compatible with any SBP operator based on the same norm matrix. The norm matrices H_{2p} are

$$H_2 = h \operatorname{diag}\left(\begin{bmatrix} \frac{1}{2} & 1 & \cdots \end{bmatrix}\right),$$
$$H_4 = h \operatorname{diag}\left(\begin{bmatrix} \frac{17}{48} & \frac{59}{48} & \frac{43}{48} & \frac{49}{48} & 1 & \cdots \end{bmatrix}\right),$$
$$H_6 = h \operatorname{diag}\left(\begin{bmatrix} \frac{13649}{43200} & \frac{12013}{8640} & \frac{2711}{4320} & \frac{5359}{4320} & \frac{7877}{8640} & \frac{43801}{43200} & 1 & \cdots \end{bmatrix}\right),$$
$$H_8 = h \operatorname{diag}\left(\begin{bmatrix} \frac{1498139}{5080320} & \frac{1107307}{725760} & \frac{20761}{80640} & \frac{1304999}{725760} & \frac{299527}{725760} & \frac{103097}{80640} & \frac{670091}{725760} & \frac{5127739}{5080320} & 1 & \cdots \end{bmatrix}\right).$$

As prescribed in Definition 3.1, the constructed OP operators satisfy $q(I_{u2v}^g) = q(I_{v2u}^g) = p + 1$ and $q(I_{u2v}^b) = q(I_{v2u}^b) = p$. These large truncation errors are localized to the boundary closures, which are comparable in size to the boundary closures of the corresponding difference operators. All constructed interpolation operators have repeating stencils of order $2p$ in the interior.

When constructing the OP operators, we made an ansatz that I_{u2v} is sparse, with nonzero boundary blocks of size $m \times n$ and an interior bandwidth d. The accuracy conditions of I_{u2v} and $I_{u2v}^\dagger$ were required to be fulfilled exactly. If the linear system that results from the accuracy conditions did not have a solution, m, n, and d were successively increased until the system became solvable. Any remaining free parameters were then used to minimize the ℓ^2-error when interpolating a sine function with 8 grid points per wavelength on the coarse grid. Figure 1 shows the sparsity pattern for the $p = 2$ case. The OP operators are available at https://bitbucket.org/martinalmquist/op_interpolation_operators.
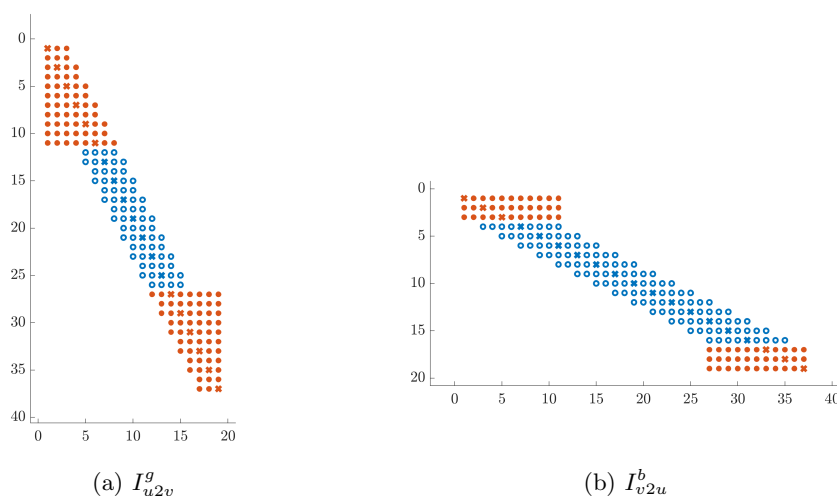

(a) I_{u2v}^g (b) I_{v2u}^b

Fig. 1. *Nonzero elements for an example pair of interpolation operators ($p = 2$). The grid ratio is 2 and the coarse grid has 20 points. Blue circles represent interior stencils, and red disks represent modified boundary stencils. (Color available online.)*

5. The second order wave equation. In this section we will use OP interpolation operators to derive stable and accurate discretizations of the wave equation with nonconforming interfaces. The new schemes are similar to those derived in [28], but with truncation errors of order $p-1$ instead of $p-2$. Since numerical experiments in [28] showed global convergence rates of order $p+1$, one may expect the new schemes to converge with rate $p+2$, which is supported by numerical experiments in section 7.

We consider the problem

$$
(5.1) \quad
\begin{aligned}
u_{tt} - c_1^2 \Delta u &= 0, \quad (x,y) \in U, \quad t \in [0, T], \\
v_{tt} - c_2^2 \Delta v &= 0, \quad (x,y) \in V, \quad t \in [0, T], \\
u - v &= 0, \quad (x,y) \in \Gamma, \quad t \in [0, T], \\
c_1^2 \tfrac{\partial u}{\partial \hat{n}_U} + c_2^2 \tfrac{\partial v}{\partial \hat{n}_V} &= 0, \quad (x,y) \in \Gamma, \quad t \in [0, T],
\end{aligned}
$$

augmented with initial data for u, u_t, v, and v_t. We assume that $c_{1,2}$ are real, positive constants. Problem (5.1) is energy-conserving and satisfies

$$
\frac{\mathrm{d}}{\mathrm{d}t} E_{wave} = 0,
$$

where

$$
(5.2) \qquad E_{wave} = \frac{1}{2} \left(\|u_t\|_U^2 + c_1^2 \|\nabla u\|_U^2 + \|v_t\|_V^2 + c_2^2 \|\nabla v\|_V^2 \right).
$$

5.1. Semidiscrete approximation. The semidiscrete approximation of (5.1) can be written as

$$
(5.3) \quad
\begin{aligned}
\mathbf{u}_{tt} - c_1^2 D_\Delta \mathbf{u} &= SAT_u, \\
\mathbf{v}_{tt} - c_2^2 D_\Delta \mathbf{v} &= SAT_v,
\end{aligned}
$$

where $SAT_{u,v}$ are penalty terms that weakly impose the interface conditions on Γ. We here make the ansatz

$$
\begin{aligned}
SAT_u = &- H_U^{-1} \left[\frac{\tau_u}{h_u} c_1^2 e_E H_U^\Gamma (e_E^T \mathbf{u} - I_{v2u}^g e_W^T \mathbf{v}) + \frac{\sigma_u}{h_v} c_2^2 e_E H_U^\Gamma I_{v2u}^b (I_{u2v}^g e_E^T \mathbf{u} - e_W^T \mathbf{v}) \right] \\
&+ H_U^{-1} \left[\frac{c_1^2}{2} d_E H_U^\Gamma (e_E^T \mathbf{u} - I_{v2u}^g e_W^T \mathbf{v}) - \frac{1}{2} e_E H_U^\Gamma (c_1^2 d_E^T \mathbf{u} + c_2^2 I_{v2u}^b d_W^T \mathbf{v}) \right],
\end{aligned}
$$

$$
\begin{aligned}
SAT_v = &- H_V^{-1} \left[\frac{\tau_v}{h_v} c_2^2 e_W H_V^\Gamma (e_W^T \mathbf{v} - I_{u2v}^g e_E^T \mathbf{u}) + \frac{\sigma_v}{h_u} c_1^2 e_W H_V^\Gamma I_{u2v}^b (I_{v2u}^g e_W^T \mathbf{v} - e_E^T \mathbf{u}) \right] \\
&+ H_V^{-1} \left[\frac{c_2^2}{2} d_W H_V^\Gamma (e_W^T \mathbf{v} - I_{u2v}^g e_E^T \mathbf{u}) - \frac{1}{2} e_W H_V^\Gamma (c_2^2 d_W^T \mathbf{v} + c_1^2 I_{u2v}^b d_E^T \mathbf{u}) \right].
\end{aligned}
$$

Assuming that the penalty parameters $\tau_{u,v}$ and $\sigma_{u,v}$ all are $\mathcal{O}(1)$, all the SATs give rise to local truncation errors that are $\mathcal{O}(h^{p-1})$.

Compared to the SBP-SAT method for conforming interfaces [18], there is an additional penalty term on each side of the interface. The second term in SAT_u evaluates the residual of the condition $u = v$ on the grid at the v-side of the interface, and then uses I_{v2u}^b to interpolate the residual to the u grid. We point out that the order of accuracy of I_{v2u}^b does not affect the order of the local truncation error of this term. The second term in SAT_v is analogous. Notice that in the case of conforming grids we may replace all interpolation operators by the identity matrix, in which case the above ansatz reduces to the one used in [18].

THEOREM 5.1. *The scheme* (5.3) *is stable if* $\sigma_v = \tau_u = \frac{\theta_u}{4\gamma_u}$ *and* $\sigma_u = \tau_v = \frac{\theta_v}{4\gamma_v}$, *where* $\theta_u, \theta_v \geq 1$.

Proof. Multiplying the first equation in (5.3) by $\mathbf{u}_t^T H_U$ yields

(5.4)
$$
\begin{aligned}
(\mathbf{u}_t, \mathbf{u}_{tt})_U = {} & c_1^2 \left(\mathbf{u}_t, D_\Delta \mathbf{u}\right)_U - \frac{\tau_u}{h_u} c_1^2 \left\langle e_E^T \mathbf{u}_t, e_E^T \mathbf{u} - I_{v2u}^g e_W^T \mathbf{v}\right\rangle_U \\
& - \frac{\sigma_u}{h_v} c_2^2 \left\langle e_E^T \mathbf{u}_t, I_{v2u}^b (I_{u2v}^g e_E^T \mathbf{u} - e_W^T \mathbf{v})\right\rangle_U \\
& + \frac{c_1^2}{2} \left\langle d_E^T \mathbf{u}_t, e_E^T \mathbf{u} - I_{v2u}^g e_W^T \mathbf{v}\right\rangle_U \\
& - \frac{1}{2} \left\langle e_E^T \mathbf{u}_t, c_1^2 d_E^T \mathbf{u} + c_2^2 I_{v2u}^b d_W^T \mathbf{v}\right\rangle_U .
\end{aligned}
$$

We now rewrite the terms one by one. By the SBP properties of D_Δ, we have

$$
c_1^2 \left(\mathbf{u}_t, D_\Delta \mathbf{u}\right)_U = c_1^2 \left\langle e_E^T \mathbf{u}_t, d_E^T \mathbf{u}\right\rangle_U - c_1^2 \left(\widetilde{D}_\nabla \mathbf{u}_t, \widetilde{D}_\nabla \mathbf{u}\right)_U .
$$

We write the first boundary integral in (5.4) as the sum of two integrals,

$$
\begin{aligned}
-\frac{\tau_u}{h_u} c_1^2 \left\langle e_E^T \mathbf{u}_t, e_E^T \mathbf{u} - I_{v2u}^g e_W^T \mathbf{v}\right\rangle_U = {} & -\frac{\tau_u}{h_u} c_1^2 \left\langle e_E^T \mathbf{u}_t, e_E^T \mathbf{u}\right\rangle_U \\
& + \frac{\tau_u}{h_u} c_1^2 \left\langle e_E^T \mathbf{u}_t, I_{v2u}^g e_W^T \mathbf{v}\right\rangle_U .
\end{aligned}
$$

We also write the second boundary integral in (5.4) as the sum of two integrals and use the adjoint property of the interpolation operators in the first of them to obtain

$$
\begin{aligned}
-\frac{\sigma_u}{h_v} c_2^2 \left\langle e_E^T \mathbf{u}_t, I_{v2u}^b (I_{u2v}^g e_E^T \mathbf{u} - e_W^T \mathbf{v})\right\rangle_U = {} & -\frac{\sigma_u}{h_v} c_2^2 \left\langle I_{u2v}^g e_E^T \mathbf{u}_t, I_{u2v}^g e_E^T \mathbf{u}\right\rangle_V \\
& + \frac{\sigma_u}{h_v} c_2^2 \left\langle e_E^T \mathbf{u}_t, I_{v2u}^b e_W^T \mathbf{v}\right\rangle_U .
\end{aligned}
$$

For the third boundary integral in (5.4), we have

$$
\frac{c_1^2}{2} \left\langle d_E^T \mathbf{u}_t, e_E^T \mathbf{u} - I_{v2u}^g e_W^T \mathbf{v}\right\rangle_U = \frac{c_1^2}{2} \left\langle d_E^T \mathbf{u}_t, e_E^T \mathbf{u}\right\rangle_U - \frac{c_1^2}{2} \left\langle d_E^T \mathbf{u}_t, I_{v2u}^g e_W^T \mathbf{v}\right\rangle_U .
$$

Using the adjoint property in the last boundary integral in (5.4) leads to

$$
\begin{aligned}
-\frac{1}{2} \left\langle e_E^T \mathbf{u}_t, c_1^2 d_E^T \mathbf{u} + c_2^2 I_{v2u}^b d_W^T \mathbf{v}\right\rangle_U = {} & -\frac{c_1^2}{2} \left\langle e_E^T \mathbf{u}_t, d_E^T \mathbf{u}\right\rangle_U \\
& - \frac{c_2^2}{2} \left\langle I_{u2v}^g e_E^T \mathbf{u}_t, d_W^T \mathbf{v}\right\rangle_V .
\end{aligned}
$$

Gathering terms, we obtain

(5.5)
$$
\begin{aligned}
(\mathbf{u}_t, \mathbf{u}_{tt})_U = {} & -\frac{c_1^2}{2} \frac{\mathrm{d}}{\mathrm{d}t} \left[\frac{\tau_u}{h_u} \langle\!\langle e_E^T \mathbf{u}\rangle\!\rangle_U^2 - \left\langle e_E^T \mathbf{u}, d_E^T \mathbf{u}\right\rangle_U + \|\widetilde{D}_\nabla \mathbf{u}\|_U^2 \right] \\
& - \frac{\sigma_u}{h_v} \frac{c_2^2}{2} \frac{\mathrm{d}}{\mathrm{d}t} \langle\!\langle I_{u2v}^g e_E^T \mathbf{u}\rangle\!\rangle_V^2 \\
& - \frac{c_1^2}{2} \left\langle d_E^T \mathbf{u}_t, I_{v2u}^g e_W^T \mathbf{v}\right\rangle_U + \frac{\tau_u}{h_u} c_1^2 \left\langle e_E^T \mathbf{u}_t, I_{v2u}^g e_W^T \mathbf{v}\right\rangle_U \\
& + \frac{\sigma_u}{h_v} c_2^2 \left\langle I_{u2v}^g e_E^T \mathbf{u}_t, e_W^T \mathbf{v}\right\rangle_V - \frac{c_2^2}{2} \left\langle I_{u2v}^g e_E^T \mathbf{u}_t, d_W^T \mathbf{v}\right\rangle_V .
\end{aligned}
$$

By repeating the procedure above for the second equation in (5.3), we arrive at a similar expression for $(\mathbf{v}_t, \mathbf{v}_{tt})_V$:

$$
\begin{aligned}
(5.6) \quad (\mathbf{v}_t, \mathbf{v}_{tt})_V = & -\frac{c_2^2}{2}\frac{\mathrm{d}}{\mathrm{d}t}\left[\frac{\tau_v}{h_v}\langle\!\langle e_W^T\mathbf{v}\rangle\!\rangle_V^2 - \langle e_W^T\mathbf{v}, d_W^T\mathbf{v}\rangle_V + \|\widetilde{D}_\nabla\mathbf{v}\|_V^2\right] \\
& -\frac{\sigma_v}{h_u}\frac{c_1^2}{2}\frac{\mathrm{d}}{\mathrm{d}t}\langle\!\langle I_{v2u}^g e_W^T\mathbf{v}\rangle\!\rangle_U^2 \\
& -\frac{c_2^2}{2}\left\langle d_W^T\mathbf{v}_t, I_{u2v}^g e_E^T\mathbf{u}\right\rangle_V + \frac{\tau_v}{h_v}c_2^2\left\langle e_W^T\mathbf{v}_t, I_{u2v}^g e_E^T\mathbf{u}\right\rangle_V \\
& +\frac{\sigma_v}{h_u}c_1^2\left\langle I_{v2u}^g e_W^T\mathbf{v}_t, e_E^T\mathbf{u}\right\rangle_U - \frac{c_1^2}{2}\left\langle I_{v2u}^g e_W^T\mathbf{v}_t, d_E^T\mathbf{u}\right\rangle_U.
\end{aligned}
$$

Adding (5.5) and (5.6) leads to

$$
\begin{aligned}
&\frac{1}{2}\frac{\mathrm{d}}{\mathrm{d}t}\left(\|\mathbf{u}_t\|_U^2 + \|\mathbf{v}_t\|_V^2 + c_1^2\|\widetilde{D}_\nabla\mathbf{u}\|_U^2 + c_2^2\|\widetilde{D}_\nabla\mathbf{v}\|_V^2\right) \\
= & -\frac{c_1^2}{2}\frac{\mathrm{d}}{\mathrm{d}t}\left[\frac{\tau_u}{h_u}\langle\!\langle e_E^T\mathbf{u}\rangle\!\rangle_U^2 - \langle e_E^T\mathbf{u}, d_E^T\mathbf{u}\rangle_U + \frac{\sigma_v}{h_u}\langle\!\langle I_{v2u}^g e_W^T\mathbf{v}\rangle\!\rangle_U^2\right] \\
& -\frac{c_2^2}{2}\frac{\mathrm{d}}{\mathrm{d}t}\left[\frac{\tau_v}{h_v}\langle\!\langle e_W^T\mathbf{v}\rangle\!\rangle_V^2 - \langle e_W^T\mathbf{v}, d_W^T\mathbf{v}\rangle_V + \frac{\sigma_u}{h_v}\langle\!\langle I_{u2v}^g e_E^T\mathbf{u}\rangle\!\rangle_V^2\right] \\
& -\frac{c_1^2}{2}\left\langle d_E^T\mathbf{u}_t, I_{v2u}^g e_W^T\mathbf{v}\right\rangle_U - \frac{c_1^2}{2}\left\langle I_{v2u}^g e_W^T\mathbf{v}_t, d_E^T\mathbf{u}\right\rangle_U \\
& +\frac{\tau_u}{h_u}c_1^2\left\langle e_E^T\mathbf{u}_t, I_{v2u}^g e_W^T\mathbf{v}\right\rangle_U + \frac{\sigma_v}{h_u}c_1^2\left\langle I_{v2u}^g e_W^T\mathbf{v}_t, e_E^T\mathbf{u}\right\rangle_U \\
& +\frac{\sigma_u}{h_v}c_2^2\left\langle I_{u2v}^g e_E^T\mathbf{u}_t, e_W^T\mathbf{v}\right\rangle_V + \frac{\tau_v}{h_v}c_2^2\left\langle e_W^T\mathbf{v}_t, I_{u2v}^g e_E^T\mathbf{u}\right\rangle_V \\
& +\frac{c_2^2}{2}\left\langle I_{u2v}^g e_E^T\mathbf{u}_t, d_W^T\mathbf{v}\right\rangle_V - \frac{c_2^2}{2}\left\langle d_W^T\mathbf{v}_t, I_{u2v}^g e_E^T\mathbf{u}\right\rangle_V.
\end{aligned}
$$

The choice $\tau_u = \sigma_v$, $\tau_v = \sigma_u$ yields

$$
(5.7) \qquad\qquad \frac{\mathrm{d}}{\mathrm{d}t}\mathcal{E}_{wave} = 0,
$$

where we have defined

$$
\mathcal{E}_{wave} = \frac{1}{2}\left(\|\mathbf{u}_t\|_U^2 + \|\mathbf{v}_t\|_V^2 + c_1^2\|\widetilde{D}_\nabla\mathbf{u}\|_U^2 + c_2^2\|\widetilde{D}_\nabla\mathbf{v}\|_V^2 + c_1^2 A_u + c_2^2 A_v\right),
$$

with

$$
\begin{aligned}
A_u = & \frac{\tau_u}{h_u}\left(\langle\!\langle e_E^T\mathbf{u}\rangle\!\rangle_U^2 - 2\left\langle e_E^T\mathbf{u}, I_{v2u}^g e_W^T\mathbf{v}\right\rangle_U + \langle\!\langle I_{v2u}^g e_W^T\mathbf{v}\rangle\!\rangle_U^2\right) \\
& -\left\langle e_E^T\mathbf{u}, d_E^T\mathbf{u}\right\rangle_U + \left\langle d_E^T\mathbf{u}, I_{v2u}^g e_W^T\mathbf{v}\right\rangle_U \\
= & \frac{\tau_u}{h_u}\langle\!\langle e_E^T\mathbf{u} - I_{v2u}^g e_W^T\mathbf{v}\rangle\!\rangle_U^2 - \left\langle d_E^T\mathbf{u}, e_E^T\mathbf{u} - I_{v2u}^g e_W^T\mathbf{v}\right\rangle_U
\end{aligned}
$$

and

$$
A_v = \frac{\tau_v}{h_v}\langle\!\langle e_W^T\mathbf{v} - I_{u2v}^g e_E^T\mathbf{u}\rangle\!\rangle_V^2 - \left\langle d_W^T\mathbf{v}, e_W^T\mathbf{v} - I_{u2v}^g e_E^T\mathbf{u}\right\rangle_V.
$$

We note that A_u and A_v are zero to the order of accuracy because $I_{v2u}^g e_W^T\mathbf{v} \simeq e_E^T\mathbf{u}$ and $I_{u2v}^g e_E^T\mathbf{u} \simeq e_W^T\mathbf{v}$. Hence, the discrete energy $\mathcal{E}_{wave}$ mimics the continuous energy E_{wave} in (5.2).

For stability it remains to prove that we can choose $\tau_{u,v}$ so that $\mathcal{E}_{wave}$ is nonnegative. By completing the squares in $A_{u,v}$ we obtain

$$A_u = \frac{\tau_u}{h_u} \left\langle\!\!\left\langle e_E^T \mathbf{u} - I_{v2u}^g e_W^T \mathbf{v} - \frac{h_u}{2\tau_u} d_E^T \mathbf{u} \right\rangle\!\!\right\rangle_U^2 - \frac{h_u}{4\tau_u} \langle\!\langle d_E^T \mathbf{u} \rangle\!\rangle_U^2$$

and

$$A_v = \frac{\tau_v}{h_v} \left\langle\!\!\left\langle e_W^T \mathbf{v} - I_{u2v}^g e_E^T \mathbf{u} - \frac{h_v}{2\tau_v} d_W^T \mathbf{v} \right\rangle\!\!\right\rangle_V^2 - \frac{h_v}{4\tau_v} \langle\!\langle d_W^T \mathbf{v} \rangle\!\rangle_V^2.$$

Because of (2.11) and (2.12), we have

$$\|\widetilde{D}_\nabla \mathbf{u}\|_U^2 \geq h_u \gamma_u \langle\!\langle d_E^T \mathbf{u} \rangle\!\rangle_U^2, \quad \|\widetilde{D}_\nabla \mathbf{v}\|_V^2 \geq h_v \gamma_v \langle\!\langle d_E^T \mathbf{v} \rangle\!\rangle_V^2.$$

We can now derive a lower bound for $\mathcal{E}_{wave}$:

$$\begin{aligned}
2\mathcal{E}_{wave} &= \|\mathbf{u}_t\|_U^2 + \|\mathbf{v}_t\|_V^2 + c_1^2 \|\widetilde{D}_\nabla \mathbf{u}\|_U^2 + c_2^2 \|\widetilde{D}_\nabla \mathbf{v}\|_V^2 + c_1^2 A_u + c_2^2 A_v \\
&\geq c_1^2 \left(\|\widetilde{D}_\nabla \mathbf{u}\|_U^2 + A_u \right) + c_2^2 \left(\|\widetilde{D}_\nabla \mathbf{v}\|_V^2 + A_v \right) \\
&\geq c_1^2 \left(h_u \gamma_u - \frac{h_u}{4\tau_u} \right) \langle\!\langle d_E^T \mathbf{u} \rangle\!\rangle_U^2 + c_2^2 \left(h_v \gamma_v - \frac{h_v}{4\tau_v} \right) \langle\!\langle d_E^T \mathbf{v} \rangle\!\rangle_V^2.
\end{aligned}$$

It follows that $\mathcal{E}_{wave} \geq 0$ if

$$\tau_u \geq \frac{1}{4\gamma_u}, \quad \tau_v \geq \frac{1}{4\gamma_v}.$$

Hence, with appropriate values of the penalty parameters, the discrete energy $\mathcal{E}_{wave}$ is a seminorm of $[\mathbf{u}, \mathbf{v}]$. The estimate (5.7) shows that $\mathcal{E}_{wave}$ is constant in time. Because $\mathcal{E}_{wave}$ contains $\|\mathbf{u}_t\|_U^2 + \|\mathbf{v}_t\|_V^2$, one can show that the solution grows at most linearly in time; see, e.g., [29]. Thus, the scheme (5.3) is stable.   □

Remark 5.2. Energy stability is guaranteed by Theorem 5.1 as long as the penalty parameters satisfy $\theta_{u,v} \geq 1$. However, the choice $\theta_{u,v} = 1$ reduces the rank of the discrete spatial operator by 1 and leads to a convergence rate lower than the ideal rate [29]. It is therefore important to set $\theta_{u,v} > 1$. Large values of $\theta_{u,v}$ may improve the accuracy, but lead to a large spectral radius of the discretization matrix and hence a small time step in explicit time stepping methods [19].

6. Three different discretizations of the Laplacian. In this section we discuss the properties of the different discrete approximations of the Laplacian that have been introduced in this paper. Recall that, with Dirichlet or Neumann boundary conditions, the continuous Laplacian is symmetric and negative semidefinite in the L^2 inner product. We shall investigate the symmetry and definiteness of the discrete Laplacians.

To suppress unnecessary notation, we assume in this section that the PDE coefficients are continuous across the domain interface Γ (the discussion applies to discontinuous coefficients too). That is, we consider (3.1) with $a = b = 1$ (the heat equation) or $a = b = i$ (the Schrödinger equation), or the wave equation (5.1) with $c_1 = c_2 = 1$. Let $\mathbf{w}^T = \begin{bmatrix} \mathbf{u}^T & \mathbf{v}^T \end{bmatrix}$, and let H denote the global quadrature defined by

$$H = \begin{bmatrix} H_U & \\ & H_V \end{bmatrix}.$$

The scheme (3.2) can be written in the forms

$$\mathbf{w}_t = D_h\mathbf{w}\ \text{(heat equation)}, \qquad \mathbf{w}_t = iD_s\mathbf{w}\ \text{(Schrödinger equation)},$$

where D_h and D_s are different approximations of the Laplacian, including the SATs for the interface conditions. For stability, the symmetric parts of HD_h and iHD_s must be negative semidefinite. The penalty parameters in (3.6) are such that HD_h is nonsymmetric but has a negative semidefinite symmetric part, while HD_s is symmetric but (in all the cases we have investigated) indefinite.

Similarly, the scheme (5.3) can be written as

$$(6.1) \qquad \mathbf{w}_{tt} = D_w\mathbf{w}\ \text{(wave equation)},$$

where D_w is the third type of approximation of the Laplacian, including the SATs for the interface conditions. Scheme (6.1) is stable if D_w is symmetric and negative semidefinite in the discrete inner product. The penalty parameters derived in Theorem 5.1 ensure precisely this. Hence, D_w mimics both of these properties of the continuous Laplacian. Note also that neither of the schemes

$$\mathbf{w}_{tt} = D_h\mathbf{w}, \quad \mathbf{w}_{tt} = D_s\mathbf{w}$$

is a stable discretization of the wave equation, but

$$\mathbf{w}_t = D_w\mathbf{w} \quad \text{and} \quad \mathbf{w}_t = iD_w\mathbf{w}$$

are stable discretizations of the heat and Schrödinger equations. So, for the heat and Schrödinger equations, we have two possible discrete Laplacians. While D_h and D_s are simple in the sense that they involve fewer penalty terms, one might argue that D_w could be a better discretization of the Laplacian since it too is symmetric and negative semidefinite. In section 7, we show that it can be beneficial to use D_w in place of D_s when discretizing the Schrödinger equation, because it leads to smaller errors and smoother convergence behavior.

7. Numerical experiments. In this section we present numerical experiments with the heat, Schrödinger, and wave equations. We use narrow-stencil diagonal-norm SBP operators [20] of interior orders $2p = 4$ and $2p = 6$ to approximate the spatial derivatives. We compare the new interface treatment based on OP interpolation operators with previous approaches that use only one pair of interpolation operators and hence suffer from accuracy reduction. For the non-OP schemes, we use interpolation operators developed by Mattsson and Carpenter [17]. The new and old schemes are abbreviated as OP and MC, respectively. We also let $\mathbb{R}^2_L$ and $\mathbb{R}^2_R$ denote the left and right half planes, respectively.

We have also derived OP interpolation operators corresponding to order $2p = 2$. In this case, MC produces the ideal convergence rate of order two. Our experiments show that the OP approach also converges with rate two, with errors almost identical to the MC errors. As there is nothing to gain in using OP interpolation for $2p = 2$, we exclude these results to simplify the presentation.

7.1. The heat equation. We consider the heat equation

$$(7.1) \qquad \begin{aligned} u_t - \lambda_1\Delta u &= 0, & (x,y) &\in \mathbb{R}^2_L, & t &> 0, \\ v_t - \lambda_2\Delta v &= 0, & (x,y) &\in \mathbb{R}^2_R, & t &> 0, \\ u - v &= 0, & x &= 0, & t &> 0, \\ \lambda_1 u_x - \lambda_2 v_x &= 0, & x &= 0, & t &> 0, \end{aligned}$$

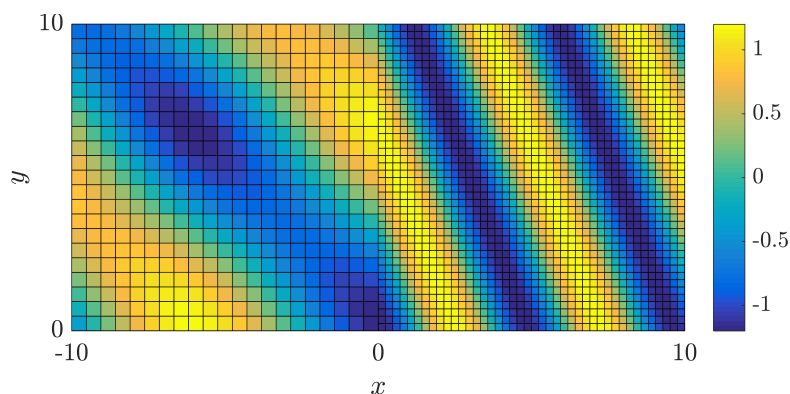FIG. 2. *The exact solution of the heat equation* (7.1) *at time* $t = 0$, *plotted on a grid of* 21×21 *points in the left block and* 41×41 *points in the right block.*

where the diffusion coefficients λ_1 and λ_2 are constant. The equation admits analytical solutions in the form

$$u = \cos(k_1 x + k_2 y)e^{-\omega t} + \gamma \cos(k_1 x - k_2 y)e^{-\omega t},$$
$$v = (1 + \gamma)\cos(kx + k_2 y)e^{-\omega t},$$

where $\omega = \lambda_1(k_1^2 + k_2^2)$, $k = \sqrt{\omega/\lambda_2 - k_2^2}$, and $\gamma = (\lambda_1 k_1 - \lambda_2 k)/(\lambda_1 k_1 + \lambda_2 k)$. We choose the diffusion coefficients $\lambda_1 = 0.1$ and $\lambda_2 = 0.025$ and set $k_1 = k_2 = 0.5$. The exact solution corresponding to these parameter values at the initial time $t = 0$ is plotted in Figure 2. In the computation we restrict the domain to $[-10, 10] \times [0, 10]$, impose Dirichlet boundary conditions at all outer boundaries, and use the exact solution to obtain initial and boundary data. The Dirichlet boundary conditions are imposed weakly by the SAT method [2].

Because the diffusion coefficient ratio is $\lambda_1/\lambda_2 = 4$, the spatial frequency in the right half plane is twice as large as that in the left half plane. To resolve this solution efficiently, we use Cartesian grids with grid sizes h_u and $h_v = 0.5h_u$ in the left and right blocks, respectively. This results in a nonconforming interface at $x = 0$ with mesh refinement ratio 1:2, as shown in Figure 2. Equation (7.1) is discretized in space by the scheme (3.2) and is integrated in time by the fourth order backward differentiation formula with a time step $\Delta t = 0.25h_v$. We set the final time $T = 2$, at which point the exact solution has the same shape as the initial solution, with the maximum amplitude diffused from 1.20 to 1.09.

In Figure 3 we plot the ℓ^2-errors of the solution at time $t = 2$. We observe that with the MC interpolation operators, the convergence rate is $p + 1$, and with the OP interpolation operators, the rate is $p + 2$, where $p = 2, 3$.

We have also performed the above experiment with the symmetric, negative semidefinite spatial discretization in (5.3) and obtained similar ℓ^2-errors and convergence rates. This suggests that the slightly simpler scheme (3.2) works well for the heat equation if solution accuracy is the primary concern. However, the symmetric discrete operator is self-adjoint just like the continuous spatial operator, and hence (5.3) is a dual-consistent scheme, while (3.2) is not [5].
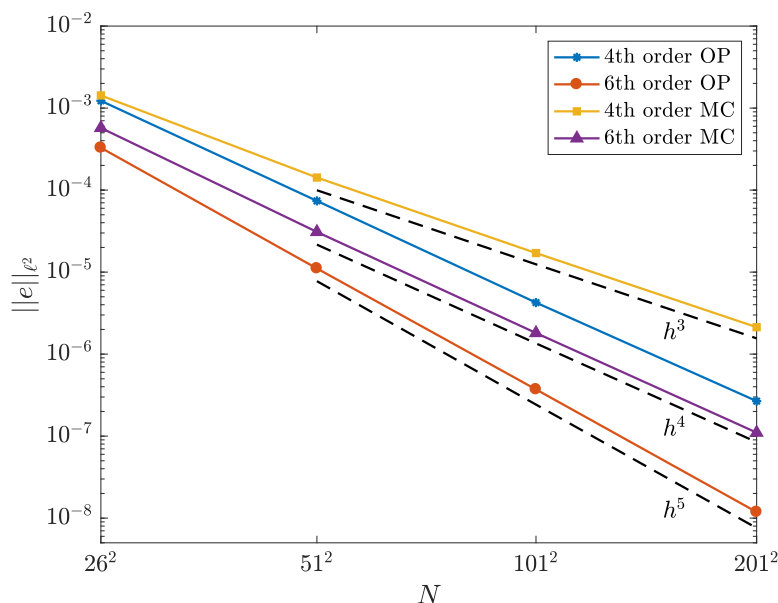
FIG. 3. *Error plot for the heat equation. OP vs. MC interpolation operators. N denotes the number of grid points in the coarse block.*

7.2. The Schrödinger equation. Consider the time dependent Schrödinger equation with a potential step,

$$
\begin{array}{llll}
\text{(7.2)} & u_t = i\Delta u, & (x,y) \in \mathbb{R}_L^2, & t > 0, \\
& v_t = i\Delta v + iV_0 v, & (x,y) \in \mathbb{R}_R^2, & t > 0, \\
& u = v, & x = 0, & t > 0, \\
& u_x = v_x, & x = 0, & t > 0,
\end{array}
$$

where V_0 is constant. Equation (7.2) admits exact solutions of the form

$$
u(x,y,t) = Ae^{i(k_1 x + k_2 y - \omega t)} + Be^{i(-k_1 x + k_2 y - \omega t)},
$$
$$
v(x,y,t) = Ce^{i(\widetilde{k}_1 x + k_2 y - \omega t)},
$$

where

$$
\omega = k_1^2 + k_2^2, \quad \widetilde{k}_1 = \sqrt{V_0 + k_1^2}, \quad B = A\frac{k_1 - \widetilde{k}_1}{k_1 + \widetilde{k}_1}, \quad C = A + B.
$$

We set $A = 1$, $V_0 = 3\pi^2$, and $k_1 = k_2 = \pi$, which yields $\omega = 2\pi^2$, $\widetilde{k}_1 = 2\pi$, $B = -\frac{1}{3}$, and $C = \frac{2}{3}$. In the computations we restrict the spatial domain to $[-1,1] \times [0,1]$. We impose Dirichlet boundary conditions and use the exact solution as initial and boundary data. Because the solution has a larger wavenumber for $x > 0$ we use two blocks with a 2:1 grid size ratio as depicted in Figure 4. We use the SBP in time method [24] with an operator based on the Gauss quadrature rule with 4 points [3] to advance the solution to the final time $T = 0.5$. The time step is chosen as $\Delta t = 0.1 h_v$. Numerical experiments indicate that this time step is small enough that the spatial errors dominate. We use fourth and sixth order spatial discretizations and compare MC with OP interpolation operators.
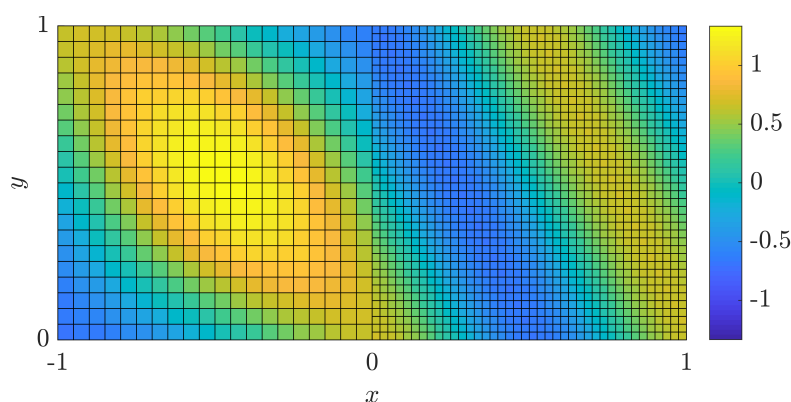
FIG. 4. *The exact solution in the experiments with the Schrödinger equation* (7.2) *at time* $t = 0$, *plotted on a grid of* 21×21 *points in the left block and* 41×41 *points in the right block.*
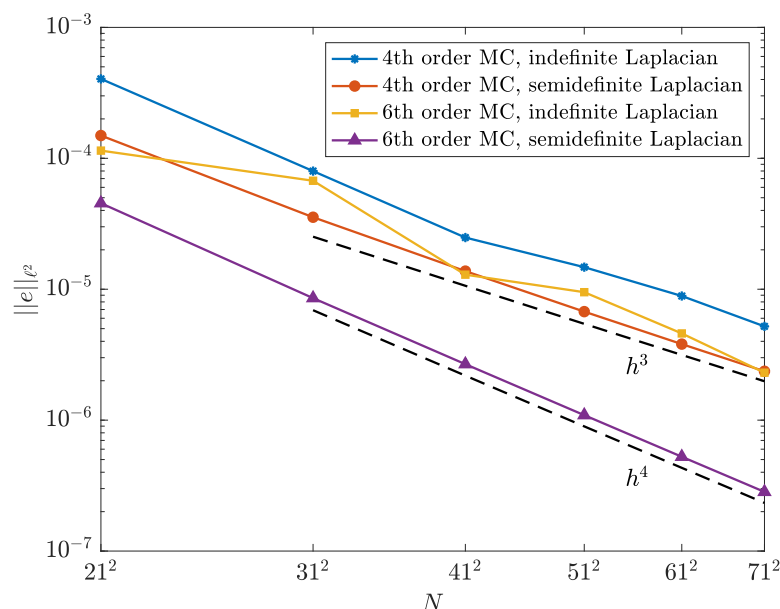

FIG. 5. *Error plot for the Schrödinger equation using MC interpolation operators, comparing semidefinite and indefinite discretizations of the Laplacian. N denotes the number of grid points in the coarse block.*

When using the indefinite discretization of the Laplacian, both MC and OP exhibit erratic convergence rates in the sixth order case; see Figures 5 and 6. Similar behavior was observed in [21]. When using the semidefinite discrete Laplacian instead, the convergence is smoother and the errors are smaller, in particular for sixth order. Hence, we propose always using the semidefinite Laplacian for the Schrödinger equation, even though the indefinite Laplacian also is stable.

Note that when switching to the semidefinite Laplacian, we changed not only the interface coupling but also the SATs that impose the Dirichlet boundary conditions on the outer boundaries. In the indefinite Laplacian we used the Dirichlet treatment in [23], and in the semidefinite Laplacian we imposed the Dirichlet conditions as in [19]. Replacing only the interface treatment or only the boundary treatment did not
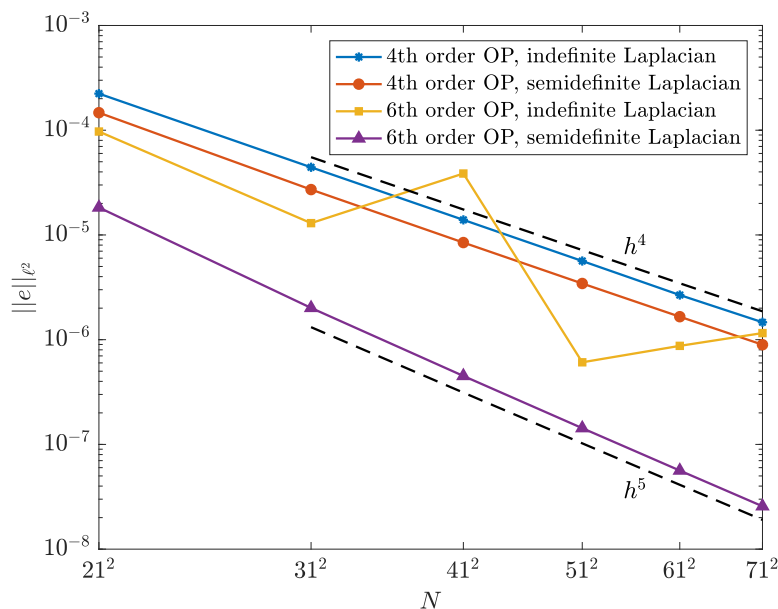
FIG. 6. *Error plot for the Schrödinger equation using OP interpolation operators, comparing semidefinite and indefinite discretizations of the Laplacian. N denotes the number of grid points in the coarse block.*

result in significantly improved convergence behavior. In the semidefinite Laplacian, we used the penalty strength 1.2 for both boundary and interface SATs.

Figure 7 compares OP with MC when using the semidefinite Laplacian. As hypothesized, MC converges with rate $p + 1$, while OP converges with rate $p + 2$.

7.3. The wave equation. We consider the wave equation

$$(7.3) \quad \begin{aligned} u_{tt} - c_1^2 \Delta u &= 0, & (x,y) \in \mathbb{R}_L^2, & \quad t > 0, \\ v_{tt} - c_2^2 \Delta v &= 0, & (x,y) \in \mathbb{R}_R^2, & \quad t > 0, \\ u - v &= 0, & x = 0, & \quad t > 0, \\ c_1^2 u_x - c_2^2 v_x &= 0, & x = 0, & \quad t > 0. \end{aligned}$$

By using Snell's law, we can derive an analytical solution in the form

$$(7.4) \quad \begin{aligned} u &= \cos(x + y - \sqrt{2}c_1 t) + k_2 \cos(x - y + \sqrt{2}c_1 t), \\ v &= (1 + k_2) \cos(k_1 x + y + \sqrt{2}c_1 t), \end{aligned}$$

where $k_1 = \sqrt{2c_1^2/c_2^2 - 1}$ and $k_2 = (c_1^2 - c_2^2 k_1)/(c_1^2 + c_2^2 k_1)$.

In the experiment, we consider a piecewise constant wave speed by setting $c_1 = 1$ and $c_2 = 0.5$. This choice makes the wavenumber in the right half plane twice as large as that in the left half plane, which can be seen in the plot of the exact solution at time $t = 0$ in Figure 8. We restrict the domain to $[-10, 10] \times [0, 10]$, impose Dirichlet boundary conditions at all outer boundaries, and use the exact solution (7.4) to obtain the initial and boundary data. To keep the number of grid points per wavelength approximately constant, we use a Cartesian mesh with mesh size h_u in the left block, and $h_v = 0.5h_u$ in the right block.

Equation (7.3) is discretized in space by the scheme (5.3), with either MC or OP interpolation operators. The Dirichlet boundary conditions are imposed weakly by
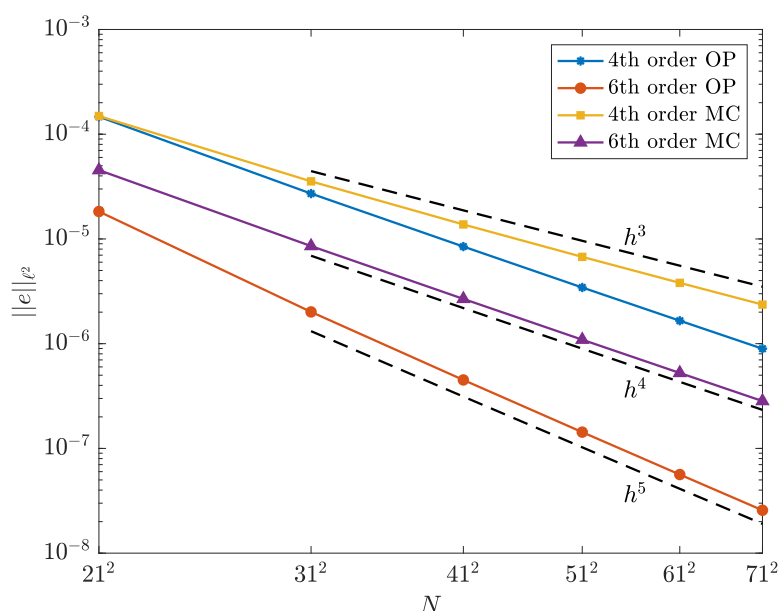
FIG. 7. *Error plot for the Schrödinger equation. OP vs. MC interpolation operators, using the semidefinite discretization of the Laplacian. N denotes the number of grid points in the coarse block.*
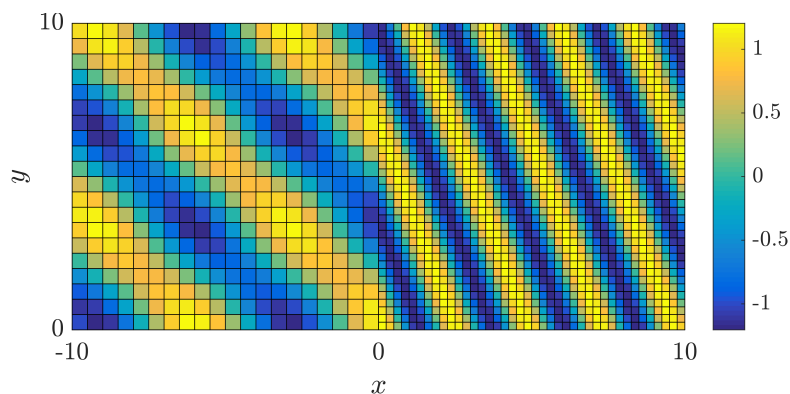

FIG. 8. *The exact solution of the wave equation (7.3) at time $t = 0$, plotted on a grid of 21×21 points in the left block and 41×41 points in the right block.*

the SAT method [1, 19]. We choose the values $\theta_u = \theta_v = 3$ for the penalty parameters in Theorem 5.1, i.e., three times the limit value required for energy stability. In the penalty terms corresponding to the Dirichlet boundary conditions, we also set the penalty parameter to three times the limit value. After rewriting the semidiscrete equation as a first order system of ODEs, we use the classical fourth order Runge–Kutta method to advance the solution to time $T = 2$. The time step is chosen as $\Delta t = 0.1 h_v$, which is small enough that the error is dominated by the spatial discretization. In the error plot in Figure 9, it is clear that the convergence rate for the scheme with the OP operators is $p+2$, whereas for MC it is $p+1$, where $p = 2, 3$.
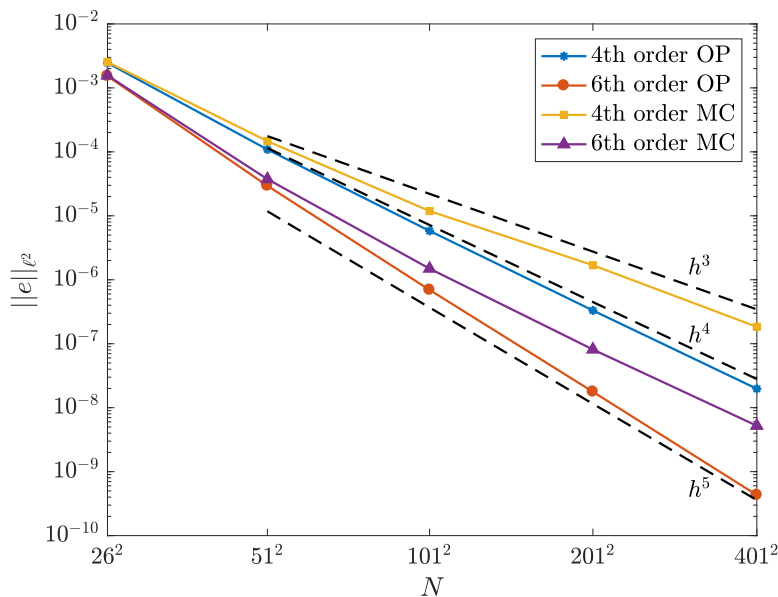
FIG. 9. *Error plot for the wave equation. OP vs. MC interpolation operators. N denotes the number of grid points in the coarse block.*

8. Conclusion. We have studied nonconforming grid interfaces for time dependent partial differential equations with second derivatives in space. To remedy previously observed decreases in convergence rates, we have introduced order-preserving (OP) interpolation operators for the nonconforming grid interfaces. The schemes based on OP operators are energy-stable and decrease the largest local truncation errors by one order compared to previous approaches. Numerical experiments demonstrate that the smaller truncation errors lead to an improvement of one order in global convergence rates.

The OP interpolation operators come in two pairs, where the two operators in a pair are the Hilbert adjoints of one another, i.e.,

$$I_{v2u}^b = (I_{u2v}^g)^\dagger, \quad I_{v2u}^g = (I_{u2v}^b)^\dagger,$$

where the inner products of the Hilbert spaces are defined by the quadrature rules that accompany the SBP operators. Let $q(I)$ denote the order of accuracy of the interpolation operator I. For traditional diagonal-norm SBP operators of interior order $2p$, it has previously been shown that $q(I) + q(I^\dagger) \leq 2p + 1$. Theorem 4.2 in this paper shows that, given two quadrature rules of order $2p$, it is always possible to obtain $q(I) + q(I^\dagger) = 2p + 1$. Moreover, the total order of $2p + 1$ may be distributed arbitrarily between I and $I^\dagger$. This guarantees that OP operators with the desired properties exist.

To summarize, we propose the following schemes. For the second order wave equation, we propose the scheme (5.3), with penalty parameters as in Theorem 5.1. For the Schrödinger equation, i.e., (3.1) with $a = i\alpha$ and $b = i\beta$, where $\alpha, \beta \in \mathbb{R}$, we propose to use the spatial operator resulting from the wave equation scheme (5.3), with c_1^2 replaced by $i\alpha$ and c_2^2 replaced by $i\beta$. For the heat equation, i.e., (3.1) with $a, b \in \mathbb{R}$, one may use either the scheme (3.2) or the spatial operator resulting from the wave equation scheme (5.3), with c_1^2 replaced by a and c_2^2 replaced by b.

REFERENCES

[1] D. Appelö and G. Kreiss, *Application of a perfectly matched layer to the nonlinear wave equation*, Wave Motion, 44 (2007), pp. 531–548, https://doi.org/10.1016/j.wavemoti.2007.01.004.

[2] J. Berg and J. Nordström, *Spectral analysis of the continuous and discretized heat and advection equation on single and multiple domains*, Appl. Numer. Math., 62 (2012), pp. 1620–1638, https://doi.org/10.1016/j.apnum.2012.05.002.

[3] P. D. Boom and D. W. Zingg, *High-order implicit time-marching methods based on generalized summation-by-parts operators*, SIAM J. Sci. Comput., 37 (2015), pp. A2682–A2709, https://doi.org/10.1137/15M1014917.

[4] M. H. Carpenter, D. Gottlieb, and S. Abarbanel, *Time-stable boundary conditions for finite-difference schemes solving hyperbolic systems: Methodology and application to high-order compact schemes*, J. Comput. Phys., 111 (1994), pp. 220–236, https://doi.org/10.1006/jcph.1994.1057.

[5] S. Eriksson, *A dual consistent finite difference method with narrow stencil second derivative operators*, J. Sci. Comput., 75 (2017), pp. 1–35, https://doi.org/10.1007/s10915-017-0569-6.

[6] D. C. Del Rey Fernández, J. E. Hicken, and D. W. Zingg, *Review of summation-by-parts operators with simultaneous approximation terms for the numerical solution of partial differential equations*, Comput. & Fluids, 95 (2014), pp. 171–196, https://doi.org/10.1016/j.compfluid.2014.02.016.

[7] L. Friedrich, D. C. Del Rey Fernández, A. R. Winters, G. J. Gassner, D. W. Zingg, and J. Hicken, *Conservative and stable degree preserving SBP operators for non-conforming meshes*, J. Sci. Comput., 75 (2018), pp. 657–686, https://doi.org/10.1007/s10915-017-0563-z.

[8] L. Friedrich, A. R. Winters, D. C. Del Rey Fernández, G. J. Gassner, M. Parsani, and M. H. Carpenter, *An entropy stable h/p non-conforming discontinuous Galerkin method with the summation-by-parts property*, J. Sci. Comput., 77 (2018), pp. 689–725, https://doi.org/10.1007/s10915-018-0733-7.

[9] L. Gao and D. Keyes, *Combining finite element and finite difference methods for isotropic elastic wave simulations in an energy-conserving manner*, J. Comput. Phys., 378 (2019), pp. 665–685, https://doi.org/10.1016/j.jcp.2018.11.031.

[10] J. Hicken and D. Zingg, *Summation-by-parts operators and high-order quadrature*, J. Comput. Appl. Math., 237 (2013), pp. 111–125, https://doi.org/10.1016/j.cam.2012.07.015.

[11] J. E. Kozdon and L. C. Wilcox, *Stable coupling of nonconforming, high-order finite difference methods*, SIAM J. Sci. Comput., 38 (2016), pp. A923–A952, https://doi.org/10.1137/15M1022823.

[12] H.-O. Kreiss and J. Oliger, *Comparison of accurate methods for the integration of hyperbolic equations*, Tellus, 24 (1972), pp. 199–215, https://doi.org/10.3402/tellusa.v24i3.10634.

[13] H.-O. Kreiss and G. Scherer, *Finite element and finite difference methods for hyperbolic partial differential equations*, in Mathematical Aspects of Finite Elements in Partial Differential Equations, Academic Press, 1974, pp. 195–212, https://doi.org/10.1016/B978-0-12-208350-1.50012-1.

[14] T. Lundquist, A. Malan, and J. Nordström, *A hybrid framework for coupling arbitrary summation-by-parts schemes on general meshes*, J. Comput. Phys., 362 (2018), pp. 49–68, https://doi.org/10.1016/j.jcp.2018.02.018.

[15] T. Lundquist and J. Nordström, *On the Suboptimal Accuracy of Summation-by-Parts Schemes with Non-conforming Block Interfaces*, Tech. Report, LiTH-MAT-R–2015/16–SE, Linköping University, 2015.

[16] K. Mattsson, *Summation by parts operators for finite difference approximations of second-derivatives with variable coefficients*, J. Sci. Comput., 51 (2012), pp. 650–682, https://doi.org/10.1007/s10915-011-9525-z.

[17] K. Mattsson and M. H. Carpenter, *Stable and accurate interpolation operators for high-order multiblock finite difference methods*, SIAM J. Sci. Comput., 32 (2010), pp. 2298–2320, https://doi.org/10.1137/090750068.

[18] K. Mattsson, F. Ham, and G. Iaccarino, *Stable and accurate wave propagation in discontinuous media*, J. Comput. Phys., 227 (2008), pp. 8753–8767, https://doi.org/10.1016/j.jcp.2008.06.023.

[19] K. Mattsson, F. Ham, and G. Iaccarino, *Stable boundary treatment for the wave equation on second-order form*, J. Sci. Comput., 41 (2009), pp. 366–383, https://doi.org/10.1007/s10915-009-9305-1.

[20] K. MATTSSON AND J. NORDSTRÖM, *Summation by parts operators for finite difference approximations of second derivatives*, J. Comput. Phys., 199 (2004), pp. 503–540, https://doi.org/10.1016/j.jcp.2004.03.001.

[21] A. NISSEN, K. KORMANN, M. GRANDIN, AND K. VIRTA, *Stable difference methods for block-oriented adaptive grids*, J. Sci. Comput., 65 (2015), pp. 486–511, https://doi.org/10.1007/s10915-014-9969-z.

[22] A. NISSEN, G. KREISS, AND M. GERRITSEN, *Stability at nonconforming grid interfaces for a high order discretization of the Schrödinger equation*, J. Sci. Comput., 53 (2012), pp. 528–551, https://doi.org/10.1007/s10915-012-9586-7.

[23] A. NISSEN, G. KREISS, AND M. GERRITSEN, *High order stable finite difference methods for the Schrödinger equation*, J. Sci. Comput., 55 (2013), pp. 173–199, https://doi.org/10.1007/s10915-012-9628-1.

[24] J. NORDSTRÖM AND T. LUNDQUIST, *Summation-by-parts in time*, J. Comput. Phys., 251 (2013), pp. 487–499, https://doi.org/10.1016/j.jcp.2013.05.042.

[25] B. STRAND, *Summation by parts for finite difference approximations for d/dx*, J. Comput. Phys., 110 (1994), pp. 47–67, https://doi.org/10.1006/jcph.1994.1005.

[26] M. SVÄRD AND J. NORDSTRÖM, *On the order of accuracy for difference approximations of initial-boundary value problems*, J. Comput. Phys., 218 (2006), pp. 333–352, https://doi.org/10.1016/j.jcp.2006.02.014.

[27] M. SVÄRD AND J. NORDSTRÖM, *Review of summation-by-parts schemes for initial–boundary-value problems*, J. Comput. Phys., 268 (2014), pp. 17–38, https://doi.org/10.1016/j.jcp.2014.02.031.

[28] S. WANG, *An improved high order finite difference method for non-conforming grid interfaces for the wave equation*, J. Sci. Comput., 77 (2018), pp. 775–792, https://doi.org/10.1007/s10915-018-0723-9.

[29] S. WANG AND G. KREISS, *Convergence of summation-by-parts finite difference methods for the wave equation*, J. Sci. Comput., 71 (2017), pp. 219–245, https://doi.org/10.1007/s10915-016-0297-3.

[30] S. WANG, A. NISSEN, AND G. KREISS, *Convergence of finite difference methods for the wave equation in two space dimensions*, Math. Comp., 87 (2018), pp. 2737–2763, https://doi.org/10.1090/mcom/3319.

[31] S. WANG, K. VIRTA, AND G. KREISS, *High order finite difference methods for the wave equation with non-conforming grid interfaces*, J. Sci. Comput., 68 (2016), pp. 1002–1028, https://doi.org/10.1007/s10915-016-0165-1.